To the Graduate Council:

I am submitting herewith a thesis written by Randal Lee Kath entitled "Petrology of the Contact Metamorphic Rocks beneath the Stillwater Complex, Montana: Conditions and Assemblages of Metamorphism." I have examined the final copy of this thesis for form and content and recommend that it be accepted in partial fulfillment of the requirements for the degree of Master of Science, with a major in Geology.

Theodore C. Labotka, Major Professor

We have read this thesis
and recommend its acceptance:

Kula C. Misra

Lawrence A. Taylor

Accepted for the Council:

Vice Provost
and Dean of The Graduate School

STATEMENT OF PERMISSION TO USE

In presenting this thesis in partial fulfillment of the requirements for a Master's of Science degree in Geology at The University of Tennessee, Knoxville, I agree that the Library shall make it available to borrowers under rules of the Library. Breif quotations from this thesis are allowable without special permission, provided that accurate acknowledgment of the source is made.

Permission for extensive quotation from or reproduction of this thesis may be granted by my major professor, or in his absence, by the Head of Interlibrary Services when, in the opinion of either, the proposed use of the material is for scholarly purposes. Any copying or use of the material in this thesis for financial gain shall not be allowed without my written permission.

Signature Randal L. Keith

Date Aug. 12, 1986

PETROLOGY OF THE CONTACT METAMORPHIC ROCKS BENEATH THE STILLWATER COMPLEX, MONTANA: CONDITIONS AND ASSEMBLAGES OF METAMORPHISM

A Thesis

Presented for the

Master of Science

Degree

The University of Tennessee, Knoxville

Randal Lee Kath

August 1986

ACKNOWLEDGMENTS

I would like to thank Dr. T. C. Labotka for introducing me to this topic and for his support and critical comments throughout this project. Most of all, I would like to thank Mr. and Mrs. R. E. Kath for their support and encouragment throughout my continuing education. The geology of the Beartooth Range is fascinating and continues to hold my interest.

ABSTRACT

The Archaean metasedimentary rocks beneath the Stillwater Igneous Complex, southwestern Montana, preserve a nearly continuous record of low-pressure facies types ranging from pyroxene hornfels through amphibole hornfels to regionally metamorphosed schists with decreasing proximity to the Stillwater contact. The pyroxene hornfels facies is characterized by the assemblage hypersthene + cordierite + garnet whereas the amphibole hornfels facies assemblages are gedrite + garnet + staurolite + cordierite, garnet + cordierite + staurolite, staurolite + anthophyllite + cordierite, and sillimanite + staurolite + cordierite. The schistose rocks contain low-grade assemblages of garnet + chlorite and andalusite + chlorite + staurolite. Due to the lack of formational names, the term Boulder River Complex is introduced to describe the metasedimentary rocks beneath the Stillwater Complex. The Boulder River Complex is composed of four mappable units: the Stillwater iron-formation, Stillwater "Blue" Quartzite, Stillwater hornfels, and the Boulder River schist. The occurrence of four-phase assemblages in the amphibole hornfels zone suggests that the chemical potential of H_2O was buffered by the rock. Isograds were mapped on the basis of the coexistence of garnet + chlorite, amphibole + staurolite + garnet + cordierite, cordierite + cummingtonite, and hypersthene.

The reactions involving chlorite are 1) garnet + chlorite = anthophyllite + staurolite + H2O and 2) chlorite = staurolite + anthophyllite + cordierite + H2O. The cummingtonite + cordierite isograd was mapped based on the following reactions: 1) staurolite + anthophyllite = garnet + cordierite + H2O and 2) garnet + anthophyllite = cummingtonite + cordierite + H2O. The hypersthene isograd involves the breakdown of cummingtonite by the following reaction: cummingtonite = hyperthene + quartz + H2O. Based on mineral equilibria, the pressure of metamorphism is bracketed between 2.0 and < 3.75 kilobars. The presence of pigeonite in the iron-formation at the base of the Stillwater Complex indicates temperatures near the contact were a minimum of 825 ^{o}C; whereas, temperatures from garnet/biotite geothermometry at a distance of 9 km range from 430^{o}C to 550^{o}C . Temperature estimates, as well as textural evidence in both the hornfels and the schists, indicate that the Stillwater Complex was emplaced at a depth of 7 to 12 km where the ambient temperature was relatively high.

TABLE OF CONTENTS

LIST OF TABLES

LIST OF FIGURES

I. INTRODUCTION

The Beartooth Mountains, which constitute a northwest-trending topographic and structural block of the Earth's crust about 128 kilometers long and 55-65 kilometers wide, are located in the Middle Rocky Mountain physiographic province east of the north-south "Wyoming" overthrust belt. The Beartooth Block is bound on the east by the Bighorn Basin, on the northeast and north by the Nye-Bowler lineament, and on the north by the Crazy Mountains syncline (Foose et al., 1961). The Precambrian terrain in the core of the Beartooth Mountains consists of predominantly granitic gneiss, pelitic schists, quartzites, amphibolites, and iron-formation, with minor irregular masses of ultramafic rocks. Located in the northeastern margin of the range is the classic Stillwater Complex.

The Stillwater Complex intruded a sequence of sedimentary rocks that includes iron-formation, quartzites, graywackes, argillites, and minor amphibolites. The contact metamorphic effects of the Stillwater Complex on the iron-formation have been studied by Labotka et al. (1982) and Vaniman et al. (1980). The effects on the pelitic rocks have been described by Page (1977), Page and Nokelberg (1972), and Weeks (1980), but the detailed petrogenesis has not been studied.

Four aspects of the petrogenesis of the metasedimentary rocks beneath the Stillwater Complex are presented. First, the equilibrium mineral assemblages are determined in order to determine the facies types for the biotite-bearing pelitic rocks. Second, the values for P and T are estimated for the pelitic assemblages to determine the metamorphic environment and its relation to the Stillwater Complex. Third, a reaction series is proposed to describe the pertinent isograds in the pelitic rocks. The mineral assemblages and mineral compositions in the hornfelses and the schists are presented in order to determine the distribution of elements among coexisting minerals in low-pressure pelitic rocks. Mineral reactions that are inferred to have happened based on a three-component AFM diagram are used to estimate the conditions of metamorphism. And, because the terrain has been suggested by various authors to be polymetamorphic, geothermometry, textural and mineralogical evidence are discussed to determine the history of the metamorphic complex.

II. REGIONAL GEOLOGY

The Precambrian crystalline core of the Beartooth Mountains has behaved as a group of huge coherent segments that are little deformed except at the edges (Lamars, 1939; Chamberlin, 1940). Lamars (1939) pointed out that the Beartooth Range is a composite uplift consisting of three well defined blocks (Fig. 1). The main part of the range, southeast of the Mill Creek-Stillwater fault zone, is the Beartooth block. The Beartooth block has been described as a rugged uplift throughout south-central Montana and adjacent Wyoming. The uplift north of the fault zone is the North Snowy block. The southwestern part of the range near Gardner is the South Snowy block. The South Snowy block is partially concealed by Tertiary volcanic rocks. During movements of the Laramide orogeny (Foose and others, 1961) these blocks were tilted. The North and South Snowy blocks slope gently to the northeast, whereas the Beartooth block slopes ~ 10 degrees southwest (Butler, 1966). The Stillwater Complex forms the northeastern boundary of the North Snowy block. A small remnant of the Stillwater Complex is located south of the Mill Creek-Stillwater fault zone in the northeast corner of the Beartooth block.

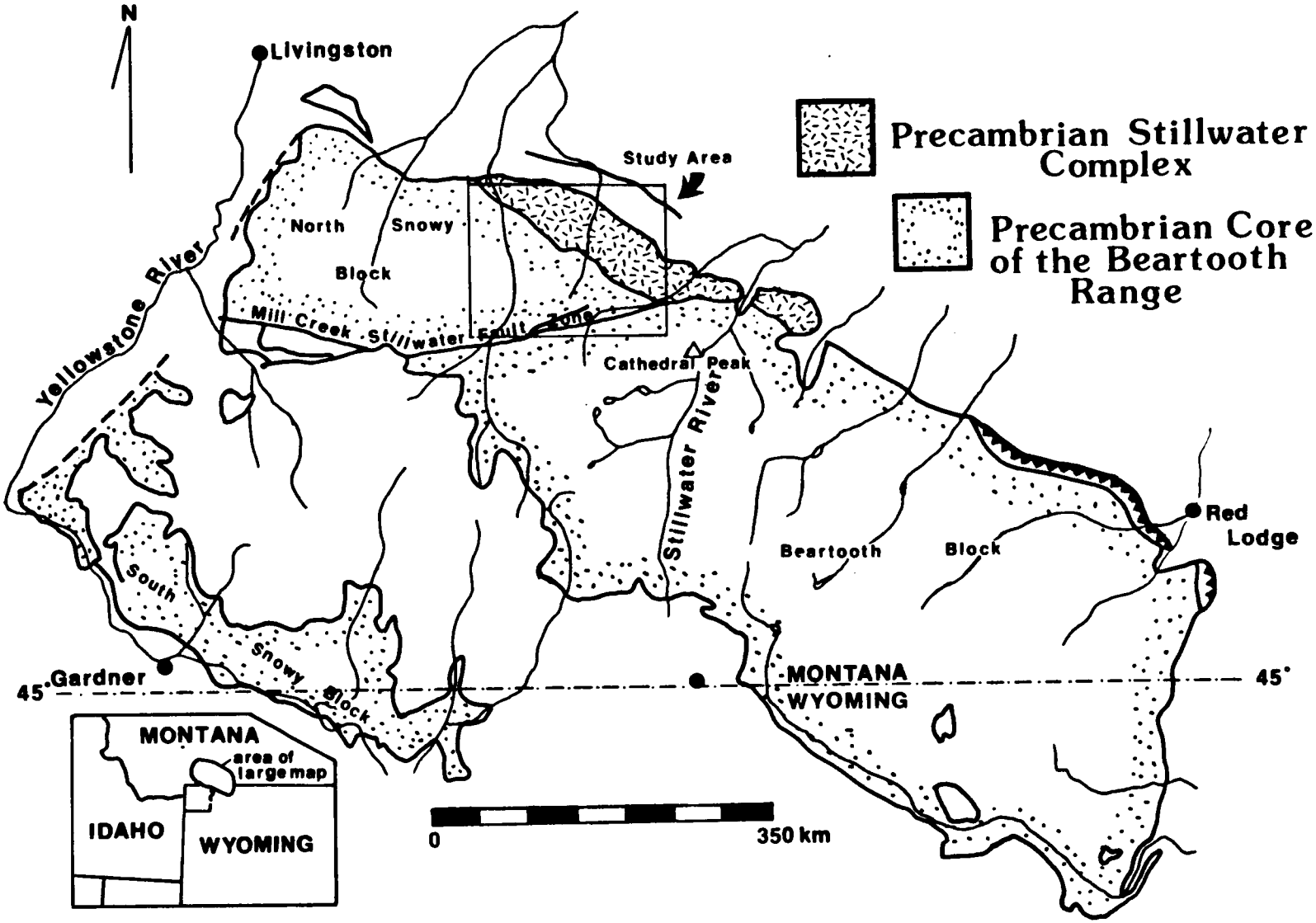

Figure 1. Index map of the Beartooth region, Montana and Wyoming (after Butler, 1966)

One of the major structural features of the Precambrian core of the Beartooth Range is the Mill Creek-Stillwater fault zone. Wilson (1936) found that the two main faults of the zone in Mill Creek basin (Fig. 1) have stratigraphic throws locally as great as ~1400 km. Published maps show the eastern end of the zone to be bifrucated (Ross and others, 1955; Jones and others, 1960); however, Butler (1966) mapped ~15 km along the supposed fault trace of the southeastern branch and found no evidence of its existence. This evidence indicates that the eastern part of the Mill Creek-Stillwater fault zone is a single fault.

Precambrian rocks crop out over an area 95 km long by 32-45 km wide in the Beartooth Mountains and are unconformably overlain by ~3000 meters of Paleozoic and Mesozoic sedimentary rocks. Granitic gneiss is the dominant rock type in most of the Beartooth Precambrian core (Eckelmann and Poldervart, 1957; Wise, 1958; Harris, 1959; Casella, 1964), but migmatite, orthoamphibolites, mafic dike rocks (Prinz, 1964), dike swarms, and metasedimentary rocks are common (Butler, 1966). The metasedimentary rocks include biotite schist, banded iron-formation, para-amphibolite, quartzite, and hornfels. Detailed rock descriptions and interpretations are given by Eckelmann and Poldervaart (1957) and Harris (1959).

A fold pattern defined by foliations and layering in the granitic gneiss and associated rocks is present over more than 120 square miles in the southeastern Beartooth Mountains (Eckelmann and Poldervaart, 1957; Wise, 1959; Harris, 1959; Cassela, 1964). Fold axes trend north-south and plunge at moderate angles to the south (Jones et al., 1960).

The Stillwater Igneous Complex, located along the northeastern margin of the Beartooth uplift, is a large differentiated mafic intrusion which represents a "gravity stratified" igneous sheet. This intrusion has been described by Hess (1960) as a deformed lopolith of Precambrian age. The exposed part of the complex is approximately 50 kilometers long and 6000 meters thick (Jones et al., 1960), in Stillwater, Park, and Sweetwater Counties Montana. Hess (1960) estimated that the exposed portion of the complex represents only 60 percent of the total thickness. The Stillwater Complex is unconformably overlain by Paleozoic sedimentary rocks, and the entire package was strongly deformed and tilted to nearly vertical during the Laramide orogeny. Both the northwestern and southeastern margins of the Stillwater Complex have been off set or truncated by faulting.

The age of the Stillwater intrusion is well constrained by both stratigraphic and isotopic techniques.

Using Sm-Nb techniques, Depalo and Wasserburg (1979) determined the age of the Stillwater Complex as 2700 my. Powell (1969), using Rb-Sr whole rocks dating techniques, determined an age of 2730 my +/- 30 my for the schistose rocks in the Boulder River area. The strong correlation between the igneous intrusive event and the metamorphic event in Boulder River strongly suggest that the heat from the intrusion reset the Rb-Sr clock or that the Stillwater Complex intruded during a regional metamorphic event.

III. GEOLOGY OF THE BOULDER RIVER VALLEY

The study area is located on the North Snowy Block (Fig. 1) in the Mt. Douglas and Mt. Cowen 15 minute quadrangles in Park, Sweetgrass, and Stillwater counties, southwestern Montana. Figure 2 shows the generalized geology of the study area in the Boulder River valley and the distribution of samples. Due to lack of formational names, the Boulder River Complex is used to describe the contact-metamorphic rocks beneath the Stillwater Igneous Complex. The Boulder River Complex consists of four distinct and mappable units: the Stillwater iron-formation, the Stillwater hornfels, the Stillwater "blue" quartzite, and the Boulder River schist. The Stillwater iron-formation and "blue" quartzite occur as concordant lenses near the contact with the Stillwater Complex. The areal distribution of the iron-formation was mapped by Page (1977) and Page et al. (1973) and other occurrences were noted during sample collection. Figure 2 illustrates the areal extent of the iron-formation. The iron-formation is usually bound on the northeast by the Stillwater Complex and on the southwest by hornfelses, although some irregular bodies of iron-formation form "islands" in the hornfelses (Fig. 2). The "blue" quartzite is not delineated on Figure 2, but it is generally associated with the iron-formation.

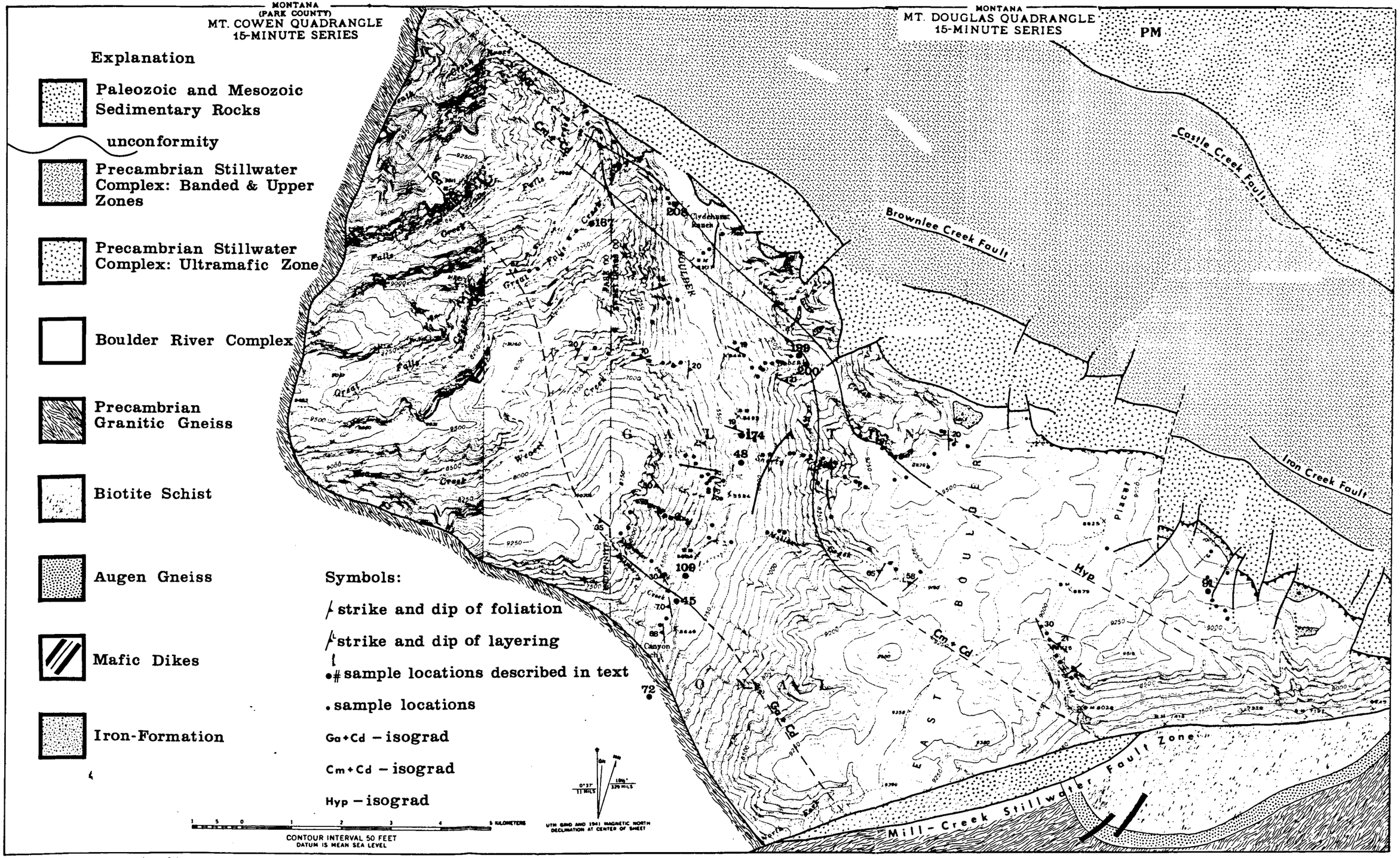

Figure 2. Sample location and generalized geologic map of the Boulder River Valley.

The Stillwater hornfels forms a 1 to 4 km-thick body that is concordant to the Stillwater Complex. Page (1977) and Page et al. (1973) mapped the entire Boulder River complex as hornfelses. The hornfels, as mapped by Page et al. (1973), consists of a orthopyroxene, amphibole, and a biotite-cordierite zone. The distribution of these zones was based on macroscopic identification of minerals. Petrographic studies by this author indicate that amphibole is a stable phase throughout the zone mapped by Page et al. (1973) as biotite-cordierite hornfels. These zones are elongate parallel to the Stillwater Complex. The Stillwater hornfels grades to the southwest into the Boulder River schist. The Boulder River schist is composed of quartzose biotite schists with various index minerals. In general, the Boulder River schist becomes more quartzose and foliated to the southwest.

The Boulder River Complex is bound on the northeast by the Stillwater Complex, to the west and southwest by Archaean granitic gneiss, and to the south by the Mill Creek-Stillwater fault zone. Structural relationships are tenuous due to the lack of distinct and continuous marker horizons within the study area; although, fold axes in the Archaean gneisses trend north-south and plunge to the south.

Throughout the study area, mafic dike rocks are present.

Both aphanitic and phaneritic varieties are seen cross-cutting the hornfelses and the schists. The apparent random orientation of the dike rocks indicates that they may not be structurally controlled in the Boulder River complex and may possibly be Laramide in age.

Foliation measurments are delineated on Figure 2. There is no apparent trend throughout the majority of the metamorphic complex; although, in the vicinity of of the major fault zones, the strike of the foliation, determined by this author and reconnaissance mapping by Page et al. (1973) in the Mt. Douglas quadrangle, is parallel to the faults. Layering , whether original or transposed, was observed and measured in two areas (Fig. 2) and is parallel to the foliation. Shear and fault zones are indicated by strongly foliated chlorite schists. These zones are seen as relatively minor features throughout the Boulder River complex, but the magnitude and abundance of these zones increases near the Mill Creek-Stillwater fault zone (Fig. 2).

Sample 78S 72 located south of the contact between the granitic gneiss and the metamorphic complex is a biotite schist that is texturally and mineralogically equivilent to the Boulder River schist. The structural relationship of this sample is not well understood. The lithologic similarity may be coincidental if the biotite schist represents a pod or lens in the granitic gneiss.

However, if the sample is a part of the Boulder River schist, it may represent a "slice" brought up from depth along the fault during initial deformation.

The Boulder River Complex is not well exposed on the east Boulder Plateau and access is difficult. The best exposure and access in located in the Boulder River valley south of McLeod, Montana. Due to lack of trails and roads, most of the samples were collected from the major drainages. Iron-formation and mafic dike rocks were not sampled, although their areal distribution and orientation was noted and is given in Figure 2.

IV. METHODS

The rocks were examined in thin section and mineral identification was aided by use of the energy dispersive system on the electron microprobe. Selected samples were analyzed with a three-spectrometer Materials Analysis Corporation 400S fully automated microprobe using natural and synthetic silicate and oxide standards. Standard operating conditions are 15 keV accelerating potential, 50 nA speciman current, 2μm beam spot, and 20 second or 20000 counts counting time. Data were reduced on-line by the method of Bence and Albee (1968) using the theoretical correction factors of Albee and Ray (1970). Precision was monitored by analyzing standards and is $< 2\%$ for major elements and $< 8\%$ for minor elements. Unknown minerals were analyzed to determine inter- and intra- granular homogenities. Several areas within each thin section were analyzed to determine compositional ranges within the area of a thin section. Sample locations are shown on Figure 2, and representative analyses are illustrated in Tables I - VII.

Table I

Representative Cordierite Analyses from the Boulder River Complex

Sample #	85S 129	85S 199	85S 109	85S 208	78S 37c	78S 14	85S 91	78S 48c	78S 16	78S 18
SiO2	47.90	48.80	48.30	48.80	50.00	48.10	49.00	48.20	48.30	49.00
TiO2	<.03	<.03	<.03	0.04	<.03	<.03	<.03	0.04	0.06	0.04
Cr2O3	<.03	<.03	<.03		0.04		0.04	<.03	<.03	<.03
Al2O3	33.20	32.90	33.00	32.50	33.80	33.70	33.60	35.50	32.60	33.20
FeO*	9.09	9.17	7.71	8.97	6.96	9.17	9.03	8.25	8.16	6.97
MnO	0.18	0.06	0.04	0.15	0.11		0.09	0.09	0.09	0.01
MgO	7.84	7.97	8.97	8.39	9.72	8.15	8.11	8.44	8.22	9.40
CaO	0.05	<.03	0.04	<.03	<.03		0.04	0.03	0.03	<.03
Na2O	0.20	0.27		0.29			0.11	0.17	0.05	<.03
K2O	0.06	<.03		0.38	<.03		0.03	0.03	<.03	<.03
Total	98.58	99.20	98.06	99.57	100.63	99.14	100.02	100.76	97.59	98.67
					Cations based on 18 oxygen					
Si	4.948	4.997	4.976	4.998	4.995	4.931	4.973	4.846	5.006	4.991
Ti	0.001	0.000	0.000	0.003	0.000	0.000	0.000	0.003	0.005	0.003
Cr	0.000	0.000	0.000		0.003		0.003	0.002	0.002	0.000
Al	4.043	3.980	4.000	3.921	3.977	4.071	4.021	4.208	3.988	3.991
Fe	0.785	0.786	0.664	0.768	0.581	0.786	0.767	0.694	0.707	0.594
Mn	0.016	0.005	0.003	0.013	0.009		0.008	0.008	0.008	0.001
Mg	1.206	1.217	1.376	1.280	1.447	1.245	1.227	1.265	1.270	1.427
Ca	0.006	0.001	0.004	0.001	0.001		0.004	0.003	0.003	0.001
Na	0.040	0.054		0.058	0.000		0.022	0.033	0.010	0.004
K	0.008	0.000		0.050	0.001		0.004	0.004	0.003	0.000
Total	11.053	11.040	11.024	11.091	11.015	11.033	11.028	11.065	11.001	11.012
Fe/Fe+Mg	0.394	0.392	0.325	0.375	0.287	0.387	0.385	0.354	0.358	0.294

* All Fe is calculated as FeO

Table II

Representative Mineral Analyses from the Boulder River Complex

	Staurolite			Hypersthene				
Sample #	85S 109	85S 174	85S 167	85S 91	78S 37C	78S 14	85S 187	78S 18
SiO2	27.50	27.00	27.80	49.70	49.10	49.70	48.70	49.00
TiO2	0.70	0.42	0.35	0.09	0.07	0.05	0.18	0.30
Cr2O3	0.23	0.06	0.14	0.06	0.19			0.50
Al2O3	54.20	54.70	54.70	1.80	2.82	1.96	2.36	4.01
FeO*	14.70	14.50	13.90	33.50	28.70	34.60	33.30	29.00
MnO	0.12	0.13	0.60	0.29	0.39		0.46	0.29
ZnO	0.14	0.28	0.21					
MgO	2.10	1.68	1.82	14.30	17.70	13.60	14.10	16.50
CaO				0.29	0.23	0.17	0.20	0.24
Na2O				<.03			<.03	<.03
Total	99.60	98.79	99.48	100.02	99.16	100.03	99.36	99.81
	Cations based on 23 oxygens			Cations based on 6 oxygens				
Si	3.767	3.730	3.805	1.953	1.909	1.958	1.930	1.891
Ti	0.072	0.044	0.036	0.003	0.002	0.001	0.005	0.009
Cr	0.025	0.007	0.015	0.002	0.006	0.000	0.000	0.015
Al	8.760	8.916	8.831	0.085	0.129	0.091	0.110	0.182
Fe	1.688	1.680	1.587	1.100	0.931	1.138	1.103	0.933
Mn	0.014	0.015	0.070	0.010	0.013	0.000	0.015	0.009
Zn	0.014	0.029	0.021					
Mg	0.429	0.346	0.371	0.836	1.022	0.798	0.835	0.951
Ca				0.012	0.010	0.007	0.008	0.010
Na				0.000	0.000	0.000	0.002	0.000
Total	14.77	14.77	14.74	4.000	4.022	3.995	4.010	4.001
Fe/Fe+Mg	0.797	0.829	0.810	0.568	0.477	0.588	0.569	0.495

* All Fe calculated as FeO

Table III

Representative Mineral Analyses from the Boulder River Complex

	Chlorite			Garnet						
Sample #	78S 45b	85S 109	85S 167	85S 91	85S 109	78S 48c	85S 199	85S 174	85S 174	78S 45b
SiO2	26.47	24.47	25.45	37.34	36.18	37.41	36.77	36.64	37.52	37.25
TiO2	0.03	0.10	0.10	0.01	0.05	0.06	0.77	0.09	0.02	0.02
Cr2O3		0.18	0.03	0.16	0.08		0.20	0.14	0.13	0.14
Al2O3	21.81	22.87	23.39	19.95	21.14	21.46	20.90	20.53	21.02	21.44
FeO*	21.62	24.50	21.64	35.27	35.64	35.73	38.18	35.78	35.54	34.13
MnO	0.01	0.04	0.27	0.78	2.18	1.72	0.76	1.45	1.59	2.11
MgO	18.05	16.33	17.63	4.56	2.68	2.76	1.79	3.34	3.14	3.45
CaO	0.45	0.06	0.02	2.32	2.23	1.21	1.34	2.15	2.34	1.39
Na2O			0.00	0.08						
K2O			0.02	0.00						
Total	88.44	88.55	88.55	100.47	100.18	100.35	100.71	100.12	101.30	99.93
	Cations based on 23 oxygens				Cations based on 12 oxygens					
Si	2.704	2.544	2.599	2.994	2.934	3.001	2.970	2.964	2.989	2.989
Ti	0.002	0.008	0.008	0.001	0.003	0.004	0.047	0.005	0.001	0.001
Cr		0.015	0.002	0.010	0.005		0.013	0.009	0.008	0.009
Al	2.627	2.803	2.816	1.886	2.021	2.029	1.990	1.958	1.974	2.028
Fe	1.847	2.130	1.848	2.365	2.418	2.397	2.579	2.421	2.368	2.290
Mn	0.001	0.004	0.023	0.053	0.150	0.117	0.052	0.099	0.107	0.143
Mg	2.748	2.530	2.683	0.545	0.324	0.330	0.215	0.403	0.373	0.413
Ca	0.049	0.007	0.002	0.199	0.194	0.104	0.116	0.186	0.200	0.119
Na			0.000	0.012						
K			0.003	0.000						
Total	9.980	10.040	9.985	8.064	8.049	7.981	7.982	8.047	8.019	7.992
Fe/Fe+Mg	0.402	0.457	0.408	0.813	0.882	0.879	0.923	0.857	0.864	0.847

* All Fe calculated as FeO

Table IV

Representative Biotite Analyses from the Boulder River Complex

Sample #	78S45	85S109	85S208	85S91	85S199	78S48C	85S129	85S129	85S187	78S37C	85S174	85S167	78S48c
SiO2	36.80	35.50	35.70	34.20	33.60	36.40	35.10	35.30	35.40	32.80	38.90	34.20	35.60
TiO2	1.53	1.67	1.70	3.13	2.48	1.26	2.87	2.86	1.81	3.58	2.44	1.27	1.73
Cr2O3		0.14		0.31	0.27		0.30	0.25		0.84	0.19	0.16	0.25
Al2O3	18.80	19.10	18.80	17.50	17.40	20.60	19.00	19.20	18.60	16.30	17.90	20.40	18.70
FeO*	16.70	18.20	18.90	19.70	20.70	18.70	18.60	18.50	19.80	17.50	17.00	17.70	19.70
MnO		<.03	0.08	0.04	0.04		0.04	0.05	0.11	<.03	0.04	0.16	<.03
MgO	12.70	11.70	10.40	9.40	10.70	10.50	9.30	10.30	10.70	14.30	10.60	11.60	10.60
CaO	<.03	<.03	<.03	<.03	<.03	<.03	<.03	<.03	<.03	<.03	<.03	<.03	<.03
Na2O			0.23	0.25	0.23		0.25	0.21	0.20		0.25	0.34	<.03
K2O	8.90	9.90	8.90	10.60	8.80	9.20	11.00	10.60	8.70	11.30	9.90	9.00	8.30
Total	95.39	96.17	94.72	95.07	94.30	96.57	96.44	97.25	95.21	96.51	97.20	94.80	95.02

Cations based on 11 oxygens

Si	2.738	2.666	2.715	2.652	2.620	2.701	2.657	2.640	2.692	2.508	2.855	2.598	2.703
Ti	0.086	0.094	0.097	0.183	0.145	0.070	0.164	0.161	0.104	0.206	0.135	0.073	0.099
Cr		0.008		0.019	0.017		0.018	0.015		0.051	0.011	0.010	0.015
Al	1.650	1.692	1.691	1.597	1.600	1.800	1.695	1.691	1.667	1.467	1.549	1.824	1.676
Fe	1.042	1.143	1.205	1.276	1.348	1.164	1.179	1.161	1.256	1.116	1.043	1.126	1.252
Mn		0.000	0.005	0.003	0.003		0.003	0.003	0.007	0.001	0.002	0.010	0.001
Mg	1.413	1.308	1.180	1.084	1.238	1.160	1.055	1.154	1.210	1.629	1.154	1.310	1.202
Ca	0.000	0.000	0.000	0.000	0.000	0.000	0.000	0.000	0.000	0.000	0.000	0.000	0.002
Na			0.034	0.038	0.035		0.037	0.030	0.029		0.036	0.050	0.003
K	0.843	0.957	0.863	1.051	0.878	0.868	1.067	1.011	0.840	1.100	0.928	0.873	0.803
Total	7.773	7.868	7.790	7.901	7.883	7.763	7.874	7.866	7.806	8.077	7.712	7.874	7.755
Fe/Fe+Mg	0.424	0.466	0.505	0.541	0.521	0.501	0.528	0.502	0.509	0.407	0.475	0.462	0.510

* All Fe calculated as FeO

Table V

Representative Plagioclase Analyses from the Boulder River Complex

Sample #	78S 45b	85S 174	385S 199	85S 208	85S 129	78S 48c	85S 109	85S 91	78S 37c	85S 167
SiO2	51.90	59.30	68.90	62.30	64.10	61.20	57.90	58.70	59.70	65.10
Al2O3	30.60	24.30	23.30	24.20	21.50	25.00	25.00	24.70	24.70	21.80
FeO	0.06	0.18	0.07	0.06	<.03		0.32	0.04	0.42	0.39
MnO			<.03	<.03						<.03
MgO		0.05	<.03	<.03	<.03			<.03	0.26	
CaO	13.70	8.40	4.60	5.30	4.20	6.20	9.40	9.50	7.30	2.50
Na2O	3.85	6.94	3.41	7.48	9.87	7.61	7.44	6.93	7.73	10.20
K2O	<.03	0.24	0.13	0.05	0.07	0.04	0.14	0.09	0.04	0.05
Total	100.20	99.41	100.48	99.46	99.76	100.05	100.13	99.95	100.18	100.02
				Cations based on 8 oxygens						
Si	2.353	2.670	2.941	2.760	2.844	2.710	2.608	2.637	2.664	2.866
Al	1.637	1.288	1.173	1.266	1.123	1.306	1.327	1.307	1.301	1.134
Fe	0.002	0.007	0.002	0.002	0.001		0.012	0.002	0.016	0.014
Mn			0.000	0.000						0.001
Mg		0.003	0.001	0.001	0.001			0.001	0.017	
Ca	0.667	0.407	0.211	0.253	0.198	0.294	0.452	0.459	0.351	0.117
Na	0.338	0.606	0.282	0.643	0.849	0.653	0.650	0.604	0.669	0.868
K	0.000	0.014	0.007	0.003	0.004	0.002	0.008	0.005	0.002	0.003
Total	4.998	4.995	4.618	4.929	5.020	4.965	5.058	5.015	5.021	5.002
An	66.34	40.17	42.82	28.25	18.93	31.01	41.04	43.21	34.42	11.89

Table VI

Representative Amphibole Analyses from the Boulder River Complex

Sample #	78S 45b	85S 208	85S 208	85S 199	85S 199	85S 174	78S 37C	85S 129	85S 129
SiO2	53.90	49.00	51.90	37.00	37.00	43.60	52.60	36.70	50.30
TiO2	0.03	0.29	0.11	0.04	0.04	0.31	0.28	0.15	0.25
Cr2O3				<.03	<.03	0.13	0.23	<.03	0.06
Al2O3	1.72	4.56	1.93	23.60	23.90	15.30	2.80	24.20	2.99
Fe2O3**	<.03	<.03	<.03	<.03	<.03	<.03	0.57	<.03	2.08
FeO*	25.10	27.50	28.70	28.10	27.80	25.60	23.90	26.80	27.10
MnO	0.45	0.60	0.61	0.15	0.13	0.34	0.35	0.62	0.54
MgO	17.00	13&10	14.00	6.92	7.02	10.90	16.90	6.68	14.10
CaO	0.43	0.21	0.13	0.13	0.16	0.49	0.44	0.12	0.22
Na2O	0.16	0.36	0.15	2.39	2.36	1.18		2.41	0.29
TOTAL	98.80	95.60	97.60	98.40	98.40	97.90	98.00	97.80	97.90
				Cations based on 23 oxygens					
Si	7.837	7.510	7.799	5.595	5.572	6.486	7.686	5.564	7.543
Ti	0.003	0.033	0.012	0.005	0.005	0.035	0.031	0.017	0.028
Cr						0.025	0.027	0.002	0.007
Al	0.295	0.824	0.342	4.201	4.256	2.687	0.476	4.313	0.529
Fe	3.050	3.518	3.605	3.551	3.500	3.193	2.918	3.394	3.404
Mn	0.055	0.078	0.078	0.019	0.017	0.043	0.043	0.080	0.069
Mg	3.682	2.994	3.140	1.558	1.576	2.421	3.688	1.508	3.151
Ca	0.067	0.034	0.021	0.021	0.026	0.078	0.069	0.019	0.035
Na	0.045	0.107	0.044	0.700	0.689	0.341		0.708	0.084
Fe3+	0.000	.000	0.000	.000	0.000	0.000	0.063	0.000	0.235
Al-IV	0.163	0.490	0.201	2.405	2.428	1.514	0.314	2.436	0.457
Al-VI	0.132	0.334	0.140	1.796	1.828	1.173	0.162	1.878	0.072
Na-M4	0.010	0.009	0.004	0.050	0.049	0.042	0.000	0.101	0.000
Fe/Fe+Mg	0.453	0.540	0.534	0.695	0.690	0.569	0.442	0.692	0.519

* All Fe calculated as FeO

** Calculated using site charge balancing

Table VII

Representative Amphibole Analyses from the Boulder River Complex

Sample #	85S 129	85S 109	78S 48c	78S48c	78S 48c	78S 48c	78S 48c	78S 48c	78S 48c	78S 16
SiO2	48.30	42.40	47.90	45.10	49.40	36.60	47.70	43.60	36.30	51.40
TiO2	0.40	0.21	0.19	0.19	0.23	0.12	0.17	0.30	<.03	0.30
Cr2O3	0.15	0.18	0.18	0.20	0.08	0.08	0.14	0.20	0.00	0.11
Al2O3	5.12	16.80	7.69	11.40	5.74	24.00	8.43	13.30	23.50	3.02
Fe2O3**	1.76	0.35								
FeO*	28.10	25.70	28.30	28.30	28.80	27.50	28.50	27.90	28.30	28.00
MnO	0.55	0.41	0.34	0.40	0.31	0.45	0.33	0.38	0.43	0.27
MgO	12.60	10.50	12.00	10.80	12.50	6.73	11.50	9.80	7.13	13.70
CaO	0.31	0.54	0.15	0.13	0.16	0.10	0.10	0.26	0.08	0.33
Na2O	0.58	1.17	0.72	0.99	0.51	2.45	0.39	1.14	2.43	0.00
TOTAL	97.90	98.20	97.60	97.60	97.70	98.00	97.20	96.90	98.10	97.10
				Cations based on 23 oxygens						
Si	7.303	6.304	7.220	6.822	7.424	5.544	7.196	6.638	5.520	7.720
Ti	0.045	0.024	0.022	0.022	0.026	0.014	0.019	0.034	0.001	0.034
Cr	0.018	0.021	0.021	0.024	0.010	0.010	0.017	0.024	0.000	0.013
Al	0.913	2.948	1.365	2.033	1.017	4.284	1.500	2.394	4.209	0.535
Fe	3.553	3.200	3.559	3.583	3.614	3.488	3.597	3.554	3.597	3.516
Mn	0.070	0.052	0.043	0.051	0.039	0.058	0.042	0.049	0.055	0.034
Mg	2.848	2.327	2.700	2.424	2.805	1.520	2.582	2.214	1.618	3.066
Ca	0.050	0.086	0.024	0.021	0.026	0.016	0.016	0.042	0.013	0.053
Na	0.170	0.338	0.210	0.290	0.149	0.720	0.114	0.336	0.717	0.000
Fe3+	0.200	0.039								
Al-IV	0.697	1.696	0.780	1.178	0.576	2.456	0.804	1.362	2.480	0.280
Al-VI	0.216	1.252	0.586	0.855	0.441	1.828	0.696	1.032	1.729	0.254
Na-M4	0.000	0.000	0.045	0.020	0.039	0.067	0.032	0.050	0.000	0.029
Fe/Fe+Mg	0.555	0.579	0.569	0.596	0.563	0.696	0.582	0.616	0.690	0.534

* All Fe calculated as FeO

** Calculated based on site charge balancing

V. MINERAL ASSEMBLAGES IN PELITIC SCHISTS

Samples were collected from more than 130 localities in the northern portion of the Mt. Douglas quadrangle in order to document the equilibrium mineral assemblages with increasing metamorphic grade. The majority of the samples were collected from the Stillwater hornfels and the Boulder River schist; although, one sample of Stillwater iron-formation and five samples of mafic dike rocks were collected. On the basis of mineral assemblages in these pelitic rocks, three isograds were mapped. The first isograd, farthest from the Stillwater Complex, marks the first appearence of garnet + cordierite. The second isograd marks the first occurrence of cummingtonite + cordierite, and the third isograd, closest to the Stillwater Complex, marks the first appearence of hypersthene.

Garnet Zone

The mineral assemblages in this zone are characterized by the presence of chlorite and include the diagnostic assemblages:

I. biotite + garnet + chlorite + orthoamphibole + plagioclase + quartz

II. biotite + andalusite + chlorite + staurolite + plagioclase + quartz

Several of these rocks contain subsets of these diagnostic assemblages. The rocks of this zone are generally fine- to medium-grained and distinctly foliated. The foliation is defined by the parallel alignment of phyllosilicates and is approximately coplanar with the compositional layering. Garnets are generally porphyroblastic and subhedral. Biotite and chlorite laths, which define the foliation, deflect around garnet porphyroblasts. This texture is characteristic throughout the garnet zone. Chlorite occurs as primary laths with quartz and feldspar inclusions and pseudomorphs that replace biotite and garnet.

As previously noted, the foliation in the rocks of the garnet zone becomes more prominent toward the south and southwest. The foliation is presumed to be metamorphic; however, an alternative is the foliation is partially or entirely caused by the Mill Creek-Stillwater fault zone and the possible fault contact between the Boulder River schist and the granitic gneiss (Fig. 2). Foliation measurements in the vicinity of Hells Canyon Ranch are near this contact and are generally coplanar. If this contact is truly a fault, the coplanar nature of the foliation would indicate that the foliation is partially or entirely fault related.

The schistose foliation near the major fault zones can be attributed, at least in part, to tectonic movement during the Laramide Orogeny. The fault controlling mechanism may be called on in the vicinity of the major faults, but it does not explain the strong foliations that are developed throughout the Boulder River schist. This topic will be discussed in a later section.

Garnet ± Cordierite Zone

Northeast of the garnet + cordierite isograd, chlorite-bearing assemblages are generally absent, except sample 85S 167; whereas, garnet + cordierite or staurolite + orthoamphibole-bearing assemblages are present. The garnet + cordierite zone is defined by the first occurrence of either garnet coexisting with cordierite or staurolite coexisting with orthoamphibole. Several diagnostic mineral assemblages observed northeast of the garnet + cordierite isograd are:

I. biotite + staurolite + orthoamphibole + garnet + quartz + plagioclase

II. biotite + staurolite + orthoamphibole + cordierite + quartz + plagioclase

III. biotite + staurolite + orthoamphibole + cordierite + garnet + quartz + plagioclase

IV. biotite + staurolite + chlorite + orthoamphibole + garnet + cordierite + quartz + plagioclase

V. biotite + staurolite + sillimanite + cordierite + quartz + plagioclase

The rocks in the garnet + cordierite zone grade northeastward from fine- to medium-grained, well foliated schists to medium- to fine-grained partially recrystallized granoblastic hornfels. The transition from schistose rocks to hornfelsic rocks is completely gradational. Due to the gradational nature of this textural zone, field determination for this "contact" was not practical. In the more schistose rocks, the foliation is defined by the preferred orientation of micas and amphibole. Progressing through this transitional zone from schistose rocks to hornfelsic rocks, the micas and amphiboles become more randomly orientated with respect to the foliation plane. As recrystallization becomes more thorough, the foliation is completely destroyed, except for relict foliations preserved as inclusions in earlier-formed minerals.

Cummingtonite + Cordierite Zone

The cummingtonite + cordierite isograd is defined by the first occurrence of cummingtonite coexisting with cordierite. The formation of cummingtonite + cordierite appears to mark the disappearance of staurolite.

Several diagnostic mineral assemblages northeast of the cummingtonite + cordierite isograd include:

I. biotite + cordierite + cummingtonite + quartz + plagioclase

II. biotite + cummingtonite + gedrite + cordierite + quartz + plagioclase

III. biotite + anthophyllite + cordierite + quartz + plagioclase

The rocks of this zone are moderately recrystallized to massive fine-grained granoblastic hornfelses. Compositional layers, which are defined by layers rich in amphibole vs. layers lacking amphibole, are preserved in some areas. This texture was noted by Page et al. (1973) during reconnaissance mapping of the Mt. Douglas Quadrangle and are indicated on Figure 2. Anthophyllite and gedrite occur as massive porphyroblasts in either bladed or radial growth forms. Cummingtonite occurs generally as elongate tabular grains and exibits good polysynthetic twinning. Cordierite forms generally large poikiloblastic grains with quartz, feldspar, and biotite inclusions. Secular twins in cordierite are present in many samples from this zone.

Hypersthene Zone

The hypersthene isograd is defined by the first appearance of hypersthene. The characteristic assemblage of this zone is the coexistence of hypersthene with cordierite and garnet. Two diagnostic mineral assemblages are observed in the hypersthene zone:

I. biotite + cordierite + hypersthene + garnet + quartz + plagioclase

II. biotite + cordierite + hypersthene + cummingtonite + quartz + plagioclase

Most rocks in this zone contain a simple assemblage of biotite + cordierite + hypersthene + quartz + plagioclase. Assemblage II marks the reaction of:

cummingtonite = hypersthene + quartz + H2O

The hypersthene zone contains rocks that have undergone complete recrystallization to fine-grained, massive granoblastic hornfels; although, the pyroxene is generally not fine-grained. In thin section, hypersthene porphyroblasts contain inclusions of biotite and plagioclase. Grains are generally large and subhedral. Retrograde alteration of hypersthene to cummingtonite and chlorite is seen in some high-grade samples. The rocks of the hypersthene zone show extensive interaction with the Stillwater Complex.

Cordierite in the hypersthene zone is generally finer-grained than cordierite from the cummingtonite + cordierite or the garnet + cordierite zone. Equilibrium grain boundaries are straight and polygonal. Characteristic secular twins are seen in the cordierite in this zone. Retrograde chlorite alteration rims are seen in the same thin sections as the retrograde chlorite of hypersthene.

VI. MINERAL CHEMISTRY

The phases of the Boulder River Complex can be represented in terms of the following oxides: SiO_2 - Cr_2O_3 - TiO_2 - FeO - MnO - ZnO - MgO - CaO - Na_2O - K_2O - H_2O. Several assumptions must be made in order to reduce the number of components for graphical representation. Since ilmenite is ubiquitous in low- and high-variance assemblages, TiO_2 is assumed to be tied-up in ilmenite. Water is considered a boundary value component (Zen, 1967). Quartz is present in all assemblages; therefore, SiO_2 is considered to be in excess. Biotite is the only K-bearing phase and is ubiquitous in all assemblages. Cr_2O_3, MnO, and ZnO occur only in trace quantities in biotite and staurolite. Plagioclase is the only Ca-bearing phase. Plagioclase and gedrite are the only Na-bearing phases. When a gedritic amphibole is present in the mineral assemblage, Na_2O must be considered an additional component. The resulting simplified system is FeO - MgO - Al_2O_3 - Na_2O (for original assumptions see Thompson, 1957).

The resulting subsystem can be presented as a three dimensional phase diagram. Since the Na_2O component is only important in gedrite-bearing assemblages, assemblages that lack gedrite may be represented as simple AFM two-dimensional phase diagrams.

Analyzed mineral assemblages in pelitic rocks of the Boulder River Complex are presented in Tables I-VII. The relative distribution of Fe and Mg between phases within any one mineral assemblage is constant. For a given assemblage, tie lines do not cross except for four-phase regions. These inconsistencies are attributed to minor changes in temperature and the activity of water. Mineral assemblages that contain gedrite show the most inconsistencies. Chemical analyses of gedrite reveal ~2 to ~4 wt. % Na_2O. The large amount of Na_2O precludes a graphical representation as a three-component system. High values for Na_2O are believed to have contributed to the formation of gedrite instead of anthophyllite; therefore, Na_2O must be treated as a separate component in order to represent gedrite-bearing assemblages graphically.

Figure 3 represents the metamorphic facies types constructed from mineral analyses from the four zones of the Boulder River Complex. Progressing from A to E represents increasing metamorphic grade. The assemblages garnet + chlorite + anthophyllite and andalusite + staurolite + chlorite (Fig. 3A) represent the chlorite + garnet zone assemblages taken from Speculator and Great Falls Creeks (Fig. 2).

Figure 3B and 3C represents assemblages from the garnet + cordierite zone.

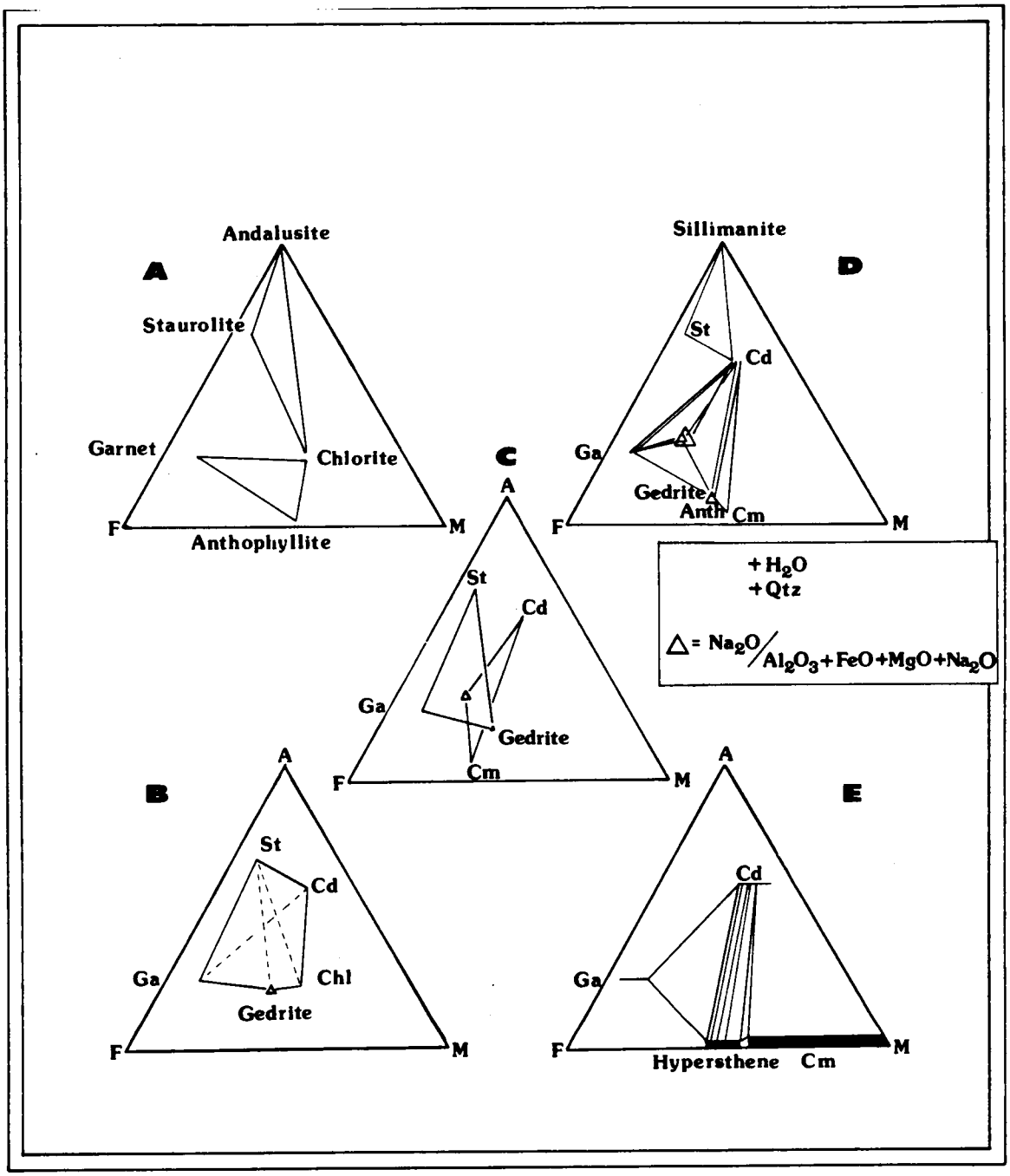

Figure 3. Metamorphic facies series constructed from mineral analyses from the pelitic rocks beneath the Stillwater complex. Progressing from A to E represents increasing metamorphic grade. All assemblages include biotite and quartz.

The five-phase assemblage (Fig. 3B) was taken from the Boulder River valley at sample location 85S 109 (Fig. 2). This low-variance assemblage contains gedrite. Gedrite on all of the succeeding diagrams is plotted as a four-component phase. The four components were normalized to 100 percent and plotted on the three-component phase diagram. The altitude of the resulting triangle represents the amount of Na2O, ie. the depth into the tetrahedron.

The crossing tie lines indicate disequilibrium, bad assumptions, or that the fluid was buffered by the rock. The relationship of chlorite in this assemblage is uncertain. In some areas of the thin section, the chlorite appears to be primary, whereas in other areas, the chlorite appears to be retrograde. If the chlorite is all retrograde, the tie-line configuration would not cross since the gedrite is within the tetrahedral volume. On the other hand, if chlorite is a primary phase, the assemblage becomes univariant which indicates that the rock had buffered the chemical potential of H2O.

The two assemblages illustrated on Figure 3C are subsets of the previous assemblage. The staurolite + garnet + gedrite assemblage is from 85S 174 (Fig. 2), and the cordierite + cummingtonite + gedrite assemblage is from sample 85S 129 (Fig. 2).

As represented on the AFM plane, the tie lines appear to be crossing; however, when plotted in the four-component system necessary when gedrite is present, the phase volumes are unique and do not intersect.

The assemblages in the garnet + cordierite zone are related to the chlorite + garnet zone by the breakdown of chlorite and the formation of either staurolite + orthoamphibole or garnet + cordierite.

In the cummingtonite + cordierite zone, the assemblages illustrated on Figure 3D are observed. Sample 85S 200 (Fig. 2) is the only assemblage that contains sillimanite. Sample 85S 48c (Fig. 2) is unique in that a range in amphibole compositions have been measured (Table VI and VII). This aspect will be discussed in a later section.

The reactions which related the garnet + cordierite zone to the cummingtonite + cordierite zone involve the breakdown of staurolite and orthoamphibole by the following reactions:

I. staurolite + anthophyllite = garnet + cordierite

II. garnet + anthophyllite = cummingtonite + cordierite.

The highest-grade assemblages observed in the Boulder River Complex are from the hypersthene zone and are graphically represented on Figure 3E. Most of the rocks of this zone contain the simple assemblage of hypersthene + cordierite + biotite + plagioclase + quartz.

Sample 85S 91 from south Iron Mountain (Fig. 2) is the only high-grade assemblage that contains garnet. Sample 78S 37c from near Chrome Mountain is the only high-grade assemblage in which cummingtonite and hypersthene coexist. The Fe/Mg ratio of the coexisting cummingtonite and hypersthene are very similar (see Figure 3E).

The reaction which relates this zone to the preceeding zone is:

cummingtonite = hypersthene + quartz + H2O.

Chlorite and garnet are the most common minerals in the low-grade rocks. Major element chemistry for chlorite and garnet are illustrated in Table III. Chlorite that coexists with garnet has a small variation in total Al content ranging from 2.60 to 2.86 cations/formula.

Garnet shows a larger range in major element content than chlorite, but this range is due to the addition of CaO and MnO components. All analyzed garnets are generally stoichiometric (Fe,Mg,Ca,Mn)3Al2Si3O12. TiO2 and Cr2O3 are present but are generally low. Compositional zonation is present with the greatest deviation between the almandine and pyrope components. Spessartine and grossular components are generally small but are found ranging up to 1 and 4 mole percent, respectively. The garnet zonation pattern is rather consistent throughout all metamorphic grades.

In general, manganese decreases from core to rim, and calcium is relatively constant within any one particular mineral assemblage. Iron is observed to increase or decrease from core to rim; although, the change in almandine component is accompanied by a change in the spessartine and grossular components. The pyrope component is generally constant from core to rim, although some garnets contain the highest pyrope component in the core.

Garnet and biotite are essentially the only Mn phases present. The variation in Mn from core to rim in the garnet may be a direct result of partitioning or fractionation of Mn between garnet and biotite. Variations in Ca content in garnet may be related to plagioclase, since plagioclase is the only other Ca-bearing phase. The chemical zonations of Mn and Ca may be reaction related. Almandine increases from 78 to 80 mole almandine component indicates that zonation in garnet is weak and of minor importance.

Biotite from the garnet + chlorite and garnet + cordierite zone contains from 0.070 to 0.117 cations Ti/formula ($\bar{}$1.26 to 2.12 wt.%) whereas biotite from the higher-grade assemblages contains from 0.079 to 0.191 cations Ti/formula ($\bar{}$1.42 to 3.26 wt.%). Although there is a minor overlapping, the Ti content appears to increase with increasing grade.

Ilmenite is believed to be the saturating Ti phase in these assemblages.

Staurolite was only analyzed in four samples. Analyses are presented in Table II. Small percentages of Zn are present but are generally less than 0.30 wt. percent. TiO2 and MnO are also present in minor quantities. The Cr content in staurolite appears to be directly proportional to the Mn content. The small amount of Ti and Mn may be due to the omnipresence of biotite and ilmenite which provide sinks for these elements.

Cordierite consists of essentially FeO, MgO, SiO2, and Al2O3. Mn, Cr, Ca, Ti, and K are present in trace quantities but are generally below the detection limits of the probe. The principal variation in cordierite chemistry is the ratio between Fe and Mg. For a particular mineral assemblage, chemical zonations are not present.

Amphibole chemistry shows the greatest variation of all observed phases. Three amphiboles are identified in the pelitic assemblages: 1) anthophyllite, 2) gedrite, and 3) cummingtonite. Generally, most assemblages contain only one amphibole phase although some contain two. Graphical representation of amphiboles from selected samples is illustrated on Figure 4 and compositional data are given in Tables VI and VII.

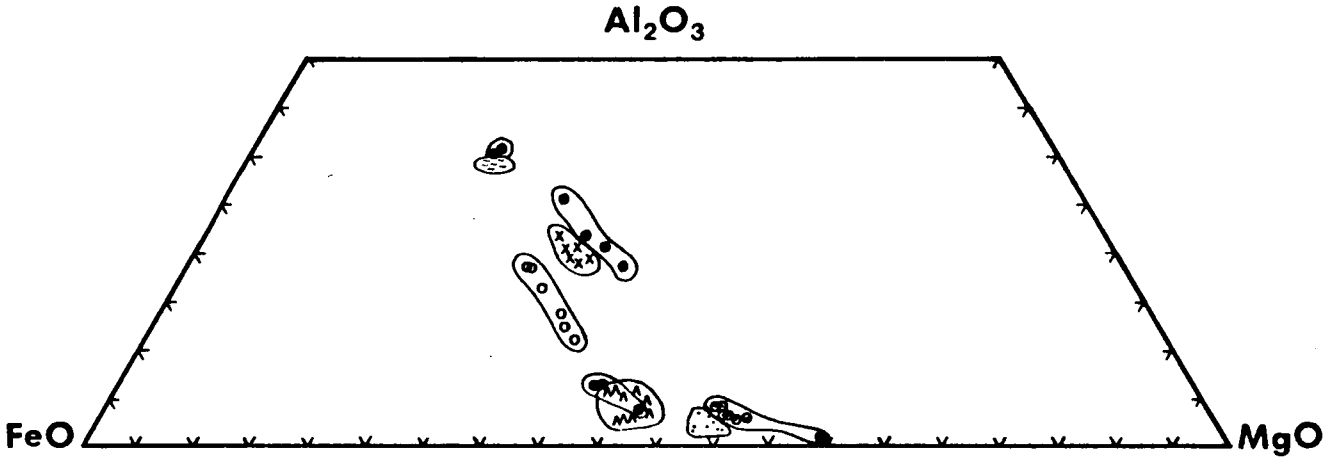

Figure 4. AFM amphibole quadralateral showing the amphibole compositions from the Boulder River Complex. Θ= 85S 129, O= 78S 48c, X= 85S 174, ●= 85S 109, ^= 85S 208, *= 78S 45b, O= 78S 37c, ~= 85S 199.

Anthophyllite generally contains less than 10 % Al2O3 whereas gedrite generally contains greater than 10 % Al2O3. Several studies have varified the presence of a miscibility gap in orthoamphiboles (Robinson and Jaffe, 1969, 1969b, 1972; Stout, 1972; Spear, 1980; Brady, 1976). Although most samples do not show two orthoamphiboles, sample 78S 48c contains a range in orthoamphibole composition. Most analyses plot in the gedrite field (Fig. 4), but an amphibole of an anthophyllite composition was observed. The sample contains no visible exsolution lamellae, and the variable composition is intergranular. This relationship may indicate that the solvus was not intersected during peak temperature conditions; orthoamphiboles from this sample may be subsolvus.

Tetrahedrally coordinatied Al in the amphiboles is plotted against octrahedrally coordinated Al + Fe3+ and against Na in Figure 5. Figure 5A represents the edenite component, whereas figure 5B is the tschermakite component. The cluster of data points above and below the scale break indicates that two modes of both types of substitution are present. The bi-modal distribution, along with amphibole analyses from sample 78S 48c, indicates the orthoamphiboles in the pelitic rocks of the Boulder River Complex are subsolvus.

Cummingtonite generally coexists with cordierite in the higher-grade assemblages.

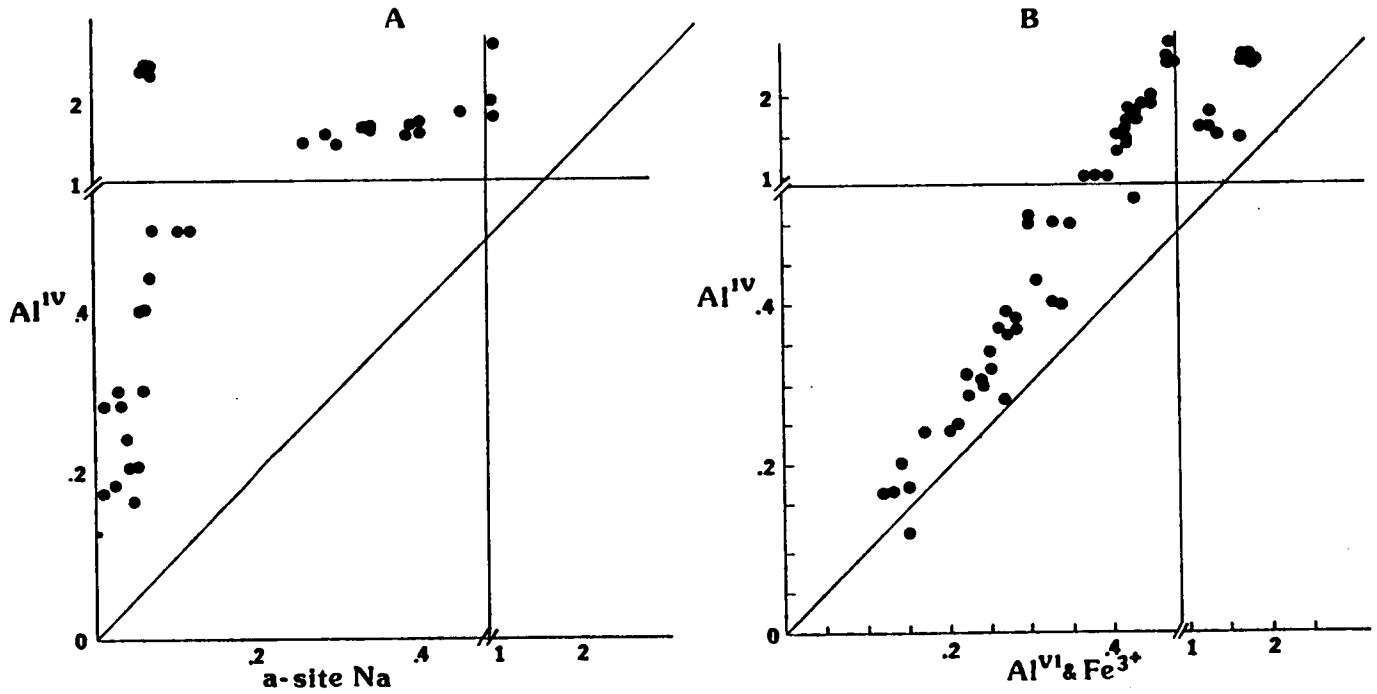

Figure 5. Plot of major amphibole substitutions in orthoamphibole. (A) Plot in molecular proportions of tetrahedral aluminum against sodium in the a-site. (B) Plot in molecular proportions of tetrahedral alumnium against the amount of octrahedral aluminum plus Fe3+.

Gedrite and anthophyllite are present in cummingtonite-bearing assemblages in samples 85S 129 and 85S 208, respectively. In both cases the orthoamphibole phase is more Mg- and Al- rich than the coexisting cummingtonite.

The principal variations in the chemistry of these minerals is the ratio of Fe to Mg. Figure 6 shows the regular distribution of Fe/Mg among coexisting phases. The systematic distribution suggests that chemical equilibrium was approached. In general, the Fe enrichment among coexisting phases is garnet > staurolite > hypersthene > anthophyllite > gedrite > cummingtonite > biotite > chlorite > cordierite. In sample 78S 37c the biotite and cummingtonite contain approximately the same Fe/Mg ratio.

Alumino-silicate polymorphs occur in these rocks in the form of sillimanite and andalusite. The sillimanite is in the form of fibrolite and comes from sample 85S 200 at the headwaters of Bobcat Creek (Fig. 2). Andalusite occurs in sample 85S 167 from Great Falls Creek (Fig. 2). Energy dispersive analyses of andalusite reveal a small but prominent Fe peak. This peak is presumed to be FeK-alpha which would represent Fe3+.

Chemographic analysis of the Boulder River Complex allows a fairly complete view of a low-pressure facies type and indicates an approach to equilibrium.

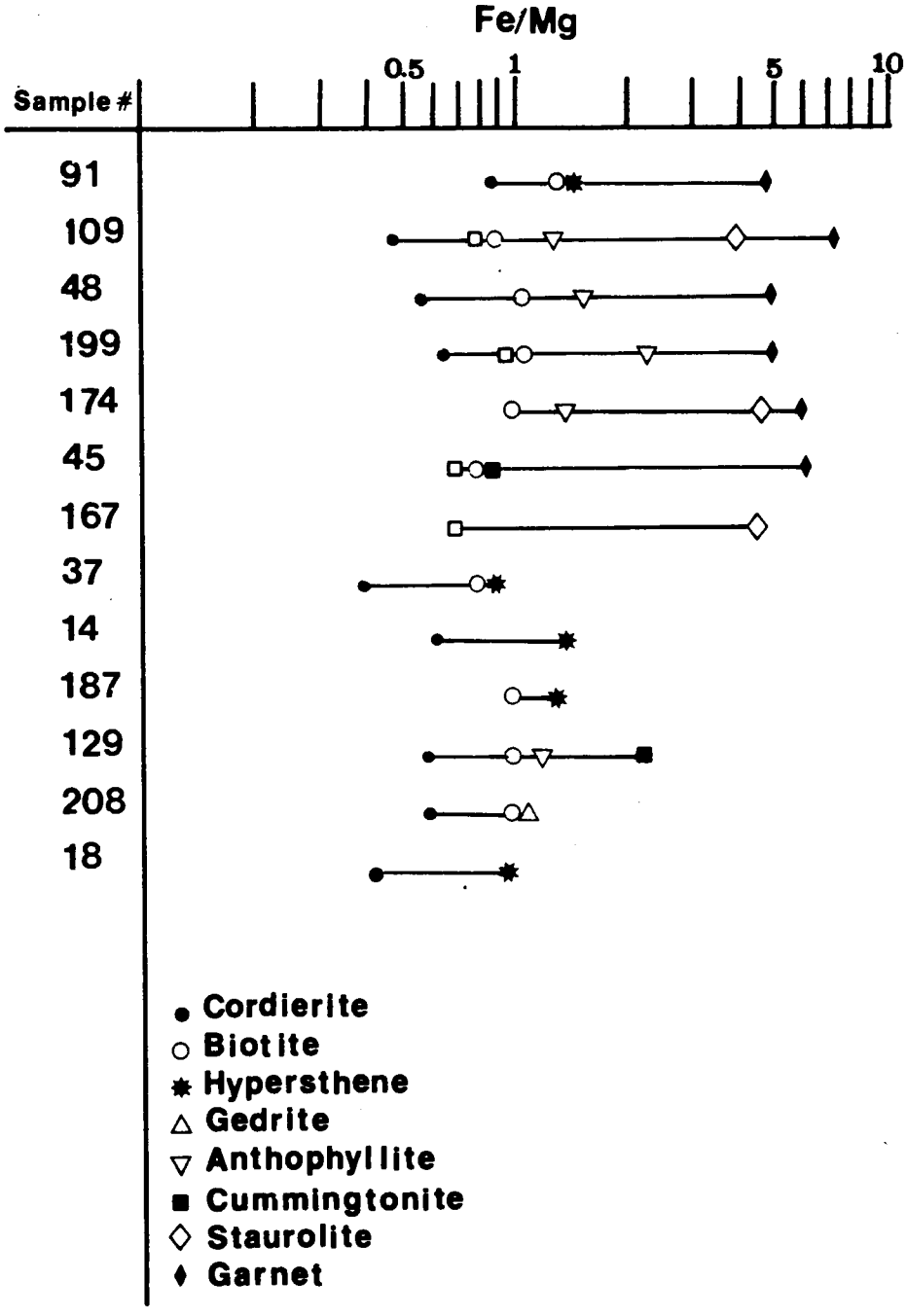

Figure 6. Semi-log plot of the systematic distribution of Fe/Mg in mafic minerals from the Boulder River Complex.

The presence of extra phases in the medium-grade rocks indicates that reactions were buffering the chemical potential of water. It is demonstrated graphically that the phases in the Boulder River Complex are reaction related.

VII. INTENSIVE PARAMETERS

Temperature and Pressure of Metamorphism

Mineral compositions in the iron-formation and pelitic rocks can be used to estimate temperature and pressure during metamorphism. The Stillwater iron-formation provides an excellent estimate of temperature at the contact with the Stillwater Complex because pigeonite occurred in assemblages from the Bluebird core and on the east side of Boulder River, near Clydehurst Ranch (Labotka, 1985). Lindsley (1983), Podpora and Lindsley (1979), and Vocke (1982) have experimentally shown that the minimum temperature of pigeonite stability is 825 ^{o}C and is independent of pressure.

Fe and Mg partitioning between coexisting garnet + biotite is temperature dependent (Ferry and Spear, 1978; A.B. Thompson, 1976; and Goldman and Albee, 1977). The partitioning of Fe and Mg between coexisting garnet + cordierite has been empirically derived by A.B. Thompson (1976). The assemblage of garnet + biotite or garnet + cordierite is rare near the contact with the Stillwater Complex. Sample 85-S-91, from south Iron Mountain, contains the assemblage of garnet + cordierite + hypersthene + biotite + plagioclase + quartz.

The garnet + biotite assemblage from this sample provides a temperature for this assemblage of 720 +/- 35 ^{o}C, using the calibration of Ferry and Spear (1978). Temperature determinations from the same sample using garnet + cordierite are in close agreement with the garnet + biotite data. Another high-grade rock that contains a favorable assemblage for Fe/Mg partitioning geothermometry is from the Cresent Creek drill core in the Mountain view area. Using the calibration of Ferry and Spear (1978), Zientek (1984) determined a temperature for this assemblage of 712 +/- 15^{o}C (Labotka, 1985).

Garnet + biotite assemblages are common in the medium- and low-grade rocks in the Boulder River valley. A sample from Shorty Creek gives a temperature of 595 ^{o}C, nearly 5 kilometers from the Stillwater Complex (Labotka, 1985). Samples from Firewater Creek, Bobcat Creek, and north of Shorty Creek (see Fig. 2) provide temperatures of ~487 +/- 58 ^{o}C, ~535 +/- 109 ^{o}C, and ~509 +/- 21 ^{o}C, respectively. Temperatures from garnet + biotite and garnet + cordierite pairs were calculated using the calibrations of Ferry and Spear (1978) and A.B. Thompson (1976), respectively. These results are tabulated in Table VIII for comparison. In general, the partitioning between the coexisting mineral pairs is systematic, and the temperature data are in close agreement.

Table VIII
Comparison of calculated temperatures using garnet/biotite and garnet/cordierite.

Sample #	Garnet Mg/Fe	Biotite Mg/Fe	Cord Mg/Fe	Calculated Temperature (K) F-S	T
85S 91 5	0.211	0.752	1.561	1027.00	940.40
85S 91 6	0.230	0.854	1.600	1008.00	961.50
85S 91 7	0.213	0.879	1.611	959.30	933.60
85S 109	0.137	1.133	2.073	729.00	754.70
85S 109	0.131	1.145	1.979	715.00	754.60
85S 109	0.143	1.194	1.990	726.80	772.70
85S 109	0.187	1.170	2.478	806.60	783.30
85S 109	0.134	1.198	2.073	709.50	749.70
85S 109	0.197	1.112	1.979	838.60	850.20
85S 109 *C	0.187	1.083	1.991	831.00	835.70
85S 109 *C	0.130	1.175	1.981	707.50	753.40
78S 48c	0.193	0.917	1.589	901.40	907.20
78S 48c	0.184	1.056	1.638	833.40	883.70
78S 48c	0.164	1.097	1.769	785.90	831.90
78S 48c	0.169	0.897	1.642	860.20	859.70
78S 48c	0.200	0.969	1.823	893.70	877.40
78S 48c	0.200	0.913	1.707	916.10	895.80
78S 48c	0.203	0.997	1.720	888.70	898.50
78S 48c	0.210	0.897	1.628	944.30	926.00
78S 48c *S	0.167	1.004		818.00	
78S 48c *S	0.177	1.021		832.70	
78S 48c *S	0.183	0.991		853.40	
78S 48c *C	0.178	1.090		812.50	
78S 48c *C	0.180	0.989		848.30	
85S 199 28	0.204	0.919	1.499	922.20	942.80
85S 199 29	0.162	0.958	1.549	823.90	864.10
85S 199 30	0.095	0.887	1.586	700.20	735.20
85S 199 31	0.084	0.919	1.576	663.30	710.90
85S 199 32	0.218	0.992		918.00	
85S 174 17	0.165	1.106		784.80	
85S 174 18	0.164	1.208		758.10	
85S 174 19	0.164	1.028		806.60	
85S 174 20	0.166	1.065		799.40	
85S 174 21	0.157	1.035		791.30	
78S 45b a	0.204	1.357		788.50	
78S 45b b	0.180	1.367		750.60	
78S 45b c	0.180	1.310		762.50	
78S 45b f	0.161	1.265		742.40	
78S 45b g	0.198	1.209		813.80	
78S 45b h	0.158	1.207		749.50	
78S 45b i	0.187	1.314		771.30	
78S 45b j	0.164	1.320		735.80	
78S 45b k	0.182	1.346		758.00	

F-S - Ferry and Spear, 1978
T - Thompson, 1976

Pressure estimates for the Boulder River Complex can be bracketed using assemblages from the Stillwater iron-formation, Stillwater hornfels, and the Boulder River schist. Lindsley (1983) determined that the lower stability limit for pigeonite was dependent on temperature and the composition of the pigeonite is pressure dependent. Vaniman et al. (1979) determined the composition of the pigeonite from the iron-formation as Wo8En23Fs69 which indicates a minimum pressure of 2 kilobars (Labotka, 1985).

Pelitic rocks containing either sillimanite or andalusite are present in the Boulder River valley. The presence of andalusite indicates a maximum pressure of 3.75 kilobars. Since the temperature in the vicinity of the andalusite-bearing samples has been determined to be 548 +/- 15 ^{o}C using garnet/biotite geothermometry, the pressure is further constrained between 2.0 and 3.2 kilobars, see Figure 7.

Further constraints on pressure can be determined from Figure 7. The experimental determination by Fonarev and Korolkov (1980) of the upper stability limit of cummingtonite is plotted on Figure 7 which shows the experimental position of the aluminosilicate triple point as experimentally determined by Holdaway (1971).

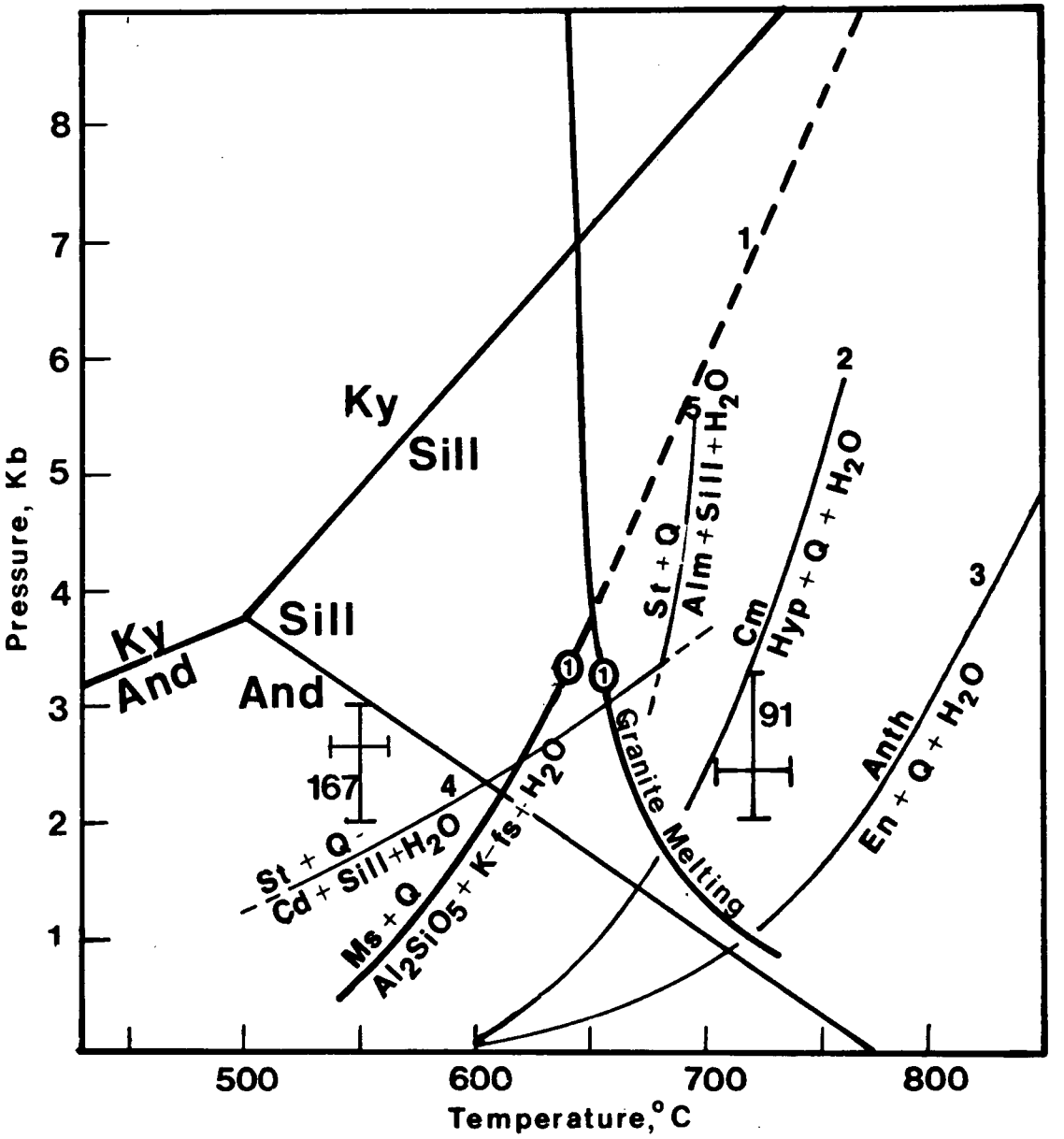

Figure 7. P-T diagram showing the alumino-silicate triple point as define by Holdaway (1971). Reaction line 1 is Ms + Q = sill + k-spar + H2O at aH2O=1. Reaction line 2 is experimentally derived by Fonarev and Korolkov (1980) which represents cummingtonite = hypersthene + quartz + H2O. Line 3 is experimentally determined by Hemley et al. (1977b) and represents anthophyllite = enststite + quartz + H2O. Reaction lines 4 and 5 are taken from Richardson (1968) and show the upper stability limits of staurolite.

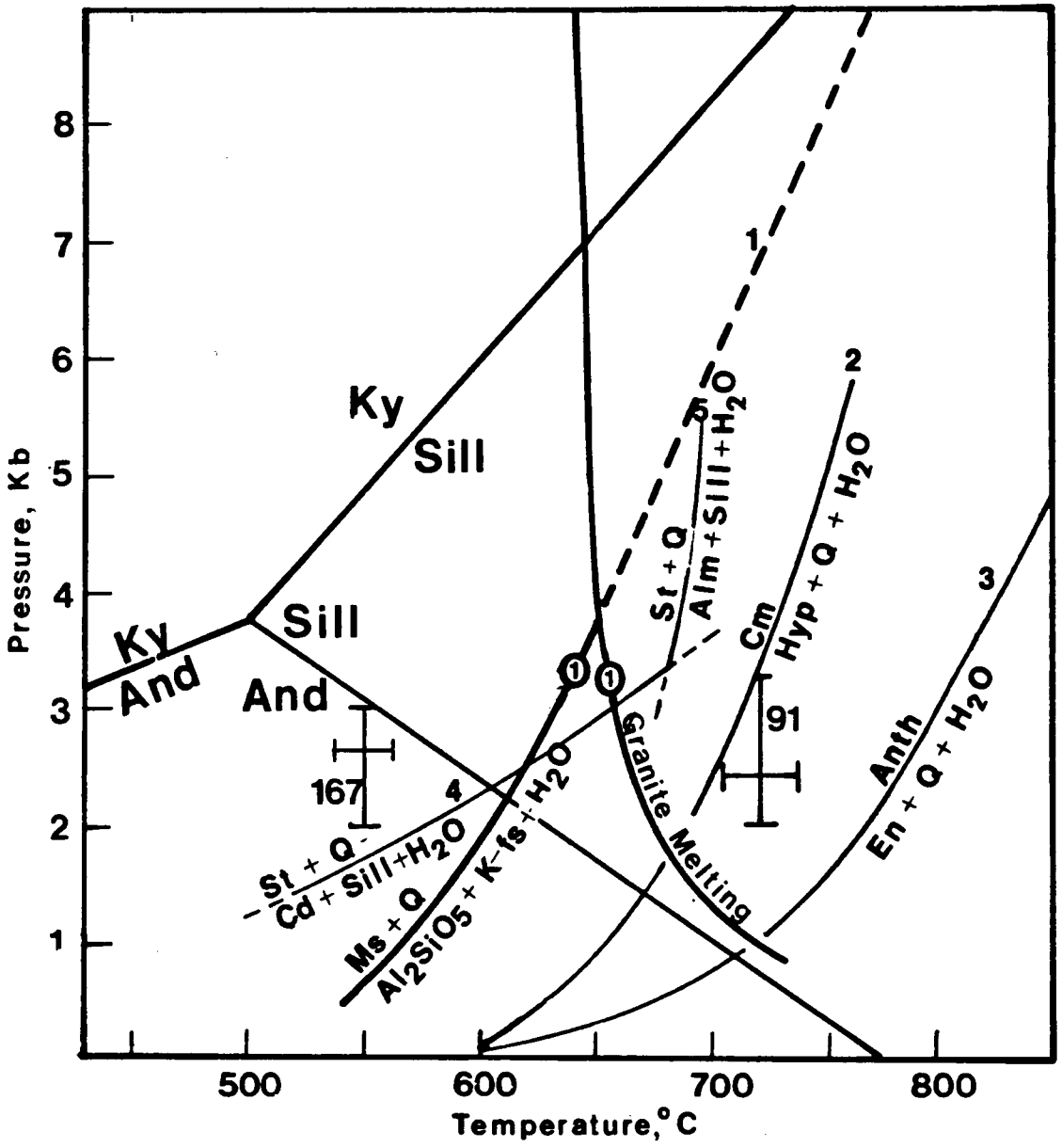

Figure 7. P-T diagram showing the alumino-silicate triple point as defined by Holdaway (1971). Reaction line 1 is Ms + Q = sill + k-spar + H2O at aH2O=1. Reaction line 2 is experimentally derived by Fonarev and Korolkov (1980) which represents cummingtonite = hypersthene + quartz + H2O. Line 3 is experimentally determined by Hemley et al. (1977b) and represents anthophyllite = ensstite + quartz + H2O. Reaction lines 4 and 5 are taken from Richardson (1968) and show the upper stability limits of staurolite.

The garnet/biotite temperature from the hypersthene assemblage in sample 85S 91 from south Iron Mountain constrains the pressure between 2.0 and 3.4 kilobars. This pressure estimate is consistent with pressures determined from the andalusite-bearing assemblage, 85S 167.

Cordierite is common to most assemblages except for the low-grade rocks. Newton (1983) and Newton and Wood (1979) discussed the temperature and pressure dependence of cordierite stability in the following reaction:

cordierite = garnet + sillimanite + quartz

The absence of coexisting garnet and sillimanite precludes an exact pressure determination. Labotka (1985) determined the composition of cordierite in a sample from Shorty Creek to be Fe/Fe+Mg = 0.37, indicating a maximum pressure of 4.0 to 5.5 kilobars, depending on the partial pressure of H20. The lack of any evidence for partial melting near the contact with the Stillwater Complex indicates that the partial pressure of H20 was low; therefore, a maximum pressure of 4.0 kilobars seems reasonable (Labotka, 1985).

VIII. DISCUSSION

The range in metamorphic grade provides a fairly continuous record of mineral facies in a low-pressure metamorphic terrain. A generalized facies series, which describes the distribution of elements between coexisting phases during metamorphism of the Boulder River Complex, is illustrated in Figure 8. The changes in mineral assemblages are indicative of prograde metamorphic reactions. Fe and Mg partitionings are systematic, suggesting that chemical equilibrium was approached. The generalized AFM reaction series for prograde metamorphic reactions is based on possible mineral assemblages. All assemblages represented on Figure 8 are not observed in the pelitic rocks due to inappropriate bulk chemistry. The relations of gedrite-bearing assemblages to the AFM assemblages are uncertain.

Based on facies types illustrated on Figure 3, the reaction series presented in Figure 8 was constructed. Figure 8A represents the stable assemblages in the low-grade rocks. With increasing grade, the facies types illustrated in Figure 8B would be stable. Figure 8B represents the same facies types as Figure 8A except that the staurolite + anthophyllite tie line is stable instead of the garnet + chlorite tie line.

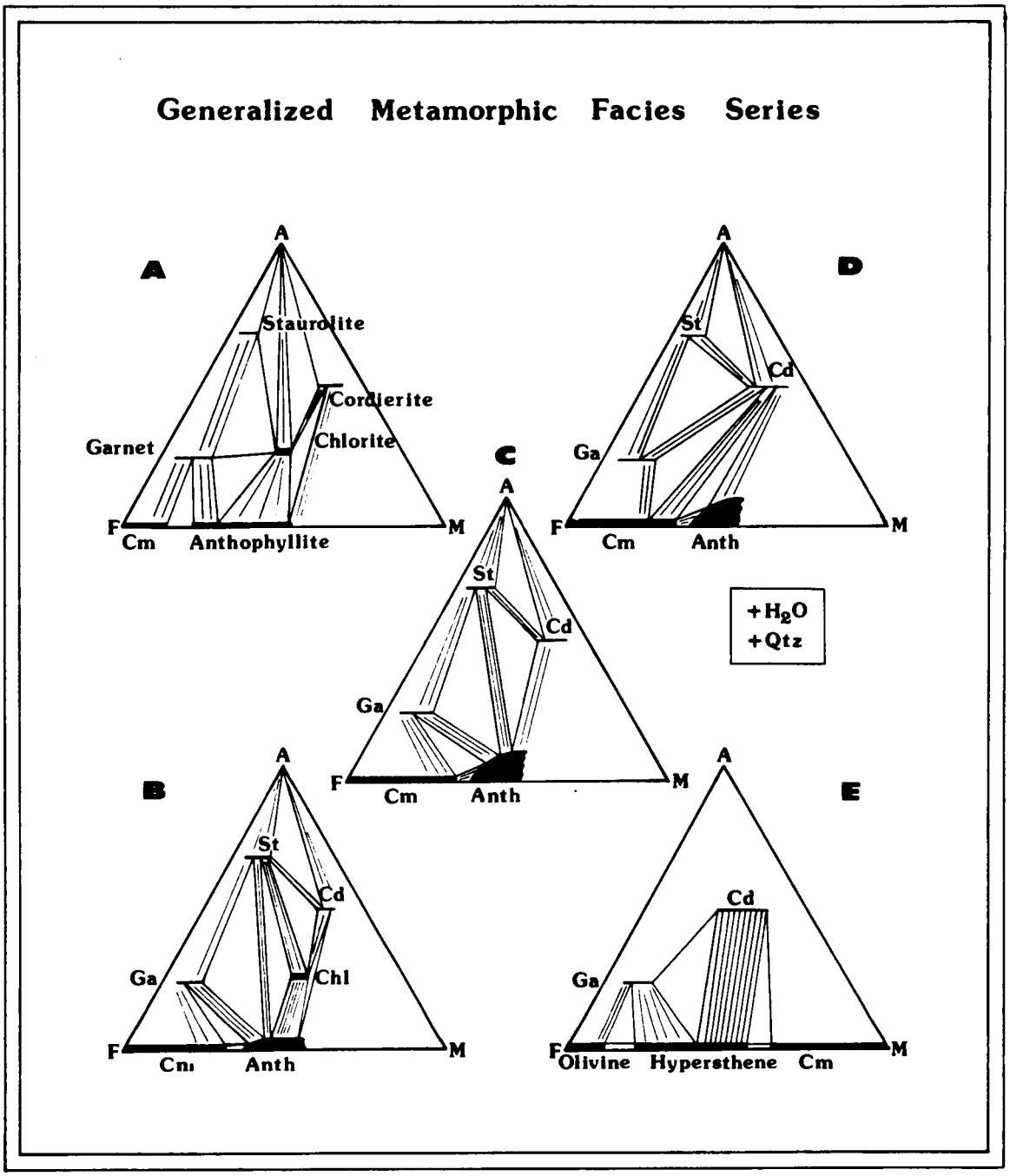

Figure 8. Generalized metamorphic facies series to represent progressive metamorphism in a low-pressure terrain.

Also progressing from Figure 8A to 8B, the aluminosilicate + chlorite tie line is no longer stable; whereas, the staurolite + cordierite tie line is stable. The reactions which relate Figure 8A to Figure B are:

(1) garnet + chlorite = staurolite + anthophyllite, and

(2) aluminosilicate + chlorite = staurolite + cordierite.

The two reactions would represent two distinct and possible isograds if the bulk composition is appropriate. Although the aluminosilicate + chlorite = staurolite + cordierite isograd is not present in the Boulder River complex, the garnet + chlorite = staurolite + anthophyllite isograd is present and is represented by the garnet + cordierite isograd delineated on Figure 2.

Facies types illustrated on Figure 8B are related to facies types illustrated on Figure 8C by a reaction involving the breakdown of chlorite. The reaction

(3) chlorite = staurolite + cordierite + anthophyllite

illustrates the last stable existence of chlorite-bearing assemblages. The transition from Figure 8B to 8C, combined with reaction (1), represents the garnet + cordierite isograd delineated on Figure 2.

Facies types illustrated on Figure 8C are the same facies types as in Figure 8D except that the garnet + cordierite and the cummingtonite + cordierite tie lines are stable instead of the staurolite + anthophyllite and garnet + anthophyllite tie lines.

It should be noted that the staurolite + anthophyllite tie line must be broken before the garnet + anthophyllite tie line can be broken. The reactions relating these facies types are

(4) staurolite + anthophyllite = garnet + cordierite, and

(5) garnet + anthophyllite = cummingtonite + cordierite.

The stable assemblages of staurolite + anthophyllite and garnet + cordierite are mutually exclusive and should not occur in the same rocks unless the chemical potential of H_2O has been buffered by the rock. Reaction (5) represents the facies type cummingtonite + cordierite. The cummingtonite + cordierite isograd is based on reaction (5).

Facies types illustrated in Figure 8E are representative of the highest-grade assemblages. The reaction which relates facies types illustrated on Figure 8D to 8E involves the breakdown of cummingtonite to form hypersthene by the following reaction:

(6) cummingtonite = hypersthene.

At even higher temperatures, the hypersthene should theoretically breakdown to form olivine. No olivine-bearing facies types are seen in the Stillwater hornfels due to inappropriate conditions.

The metamorphic isograds mapped in the Boulder River Complex are delineated on Figure 2.

Metamorphic grade increases to the northeast or as the Stillwater Complex is approached. The isograds appear to be truncated to the south by the Mill Creek-Stillwater fault zone. The highest-grade rocks occur near the Stillwater Complex in the pyroxene zone of the Stillwater hornfels. The lowest-grade rocks are found near Speculator Creek and in the head waters of Great Falls creek where chlorite-bearing assemblages are present (Fig. 2).

The facies series progresses from the garnet + chlorite zone assemblage of chlorite + garnet to a garnet + cordierite zone assemblage of garnet + staurolite + amphibole and staurolite + cordierite + amphibole to a cummingtonite + cordierite zone assemblage of cummingtonite + cordierite to a hypersthene zone assemblage of hypersthene + garnet + cordierite. The reaction sequence is based on observed mineral assemblages and compositions from Figure 3 and Tables I thru VII, respectively. The AFM components of chlorite, staurolite, anthophyllite, cummingtonite, garnet, and cordierite were used in the following mass balance calculations. Chlorite compositions used in reactions (1) and (3) were taken from samples 167 and 109, respectively. Garnet compositions used in reactions (1), (4), and (5) were taken from samples 109, 174, and 199, respectively. Staurolite compositions used in reactions (1), (3), and (4) were taken from samples 109, 174, and 167, respectively.

Anthophyllite, cordierite, and cummingtonite compositions were taken from sample 129. The following reactions represents prograde metamorphic reactions and assumes H20 is liberated with increasing grade:

(1) 9.60 garnet + 34.00 chlorite + 110.0 quartz + 1.00 albite = 10.90 staurolite + 25.00 anthophyllite + 101.0 H20

(2) aluminosilicate + chlorite + quartz = staurolite + cordierite + H20

(3) 47.5 chlorite + 196.0 quartz + 1.00 albite = 25.00 anthophyllite + 26.00 cordierite + 1.05 staurolite + 164.0 H20

(4) 36.1 staurolite + 25.00 anthophyllite + 108.0 quartz = 34.00 garnet + 67.00 cordierite + 61.00 H20

(5) 4.40 garnet + 25.00 anthophyllite + 21.00 quartz = 24.00 cummingtonite + 6.00 cordierite + 0.85 H20

(6) cummingtonite = hypersthene + quartz + H20

Reactions 1,2, and 3 represent the the transition from the garnet + chlorite zone to the garnet + cordierite zone. The isograd between these zones represents the breakdown of chlorite to form the stable coexistence of either garnet + cordierite or staurolite + orthoamphibole. The stoichiometry of the reaction products predicts the common assemblage staurolite + anthophyllite + cordierite, northeast of the garnet + cordierite isograd.

Field occurrences of these phases correlates with this prediction. Many univariant assemblages are observed in the garnet + cordierite zone. These assemblages contain all four phases of reaction (3). The aspect of univariant assemblages in the garnet + cordierite zone will be discussed in a later section.

Reaction (3) takes place throughout the garnet + cordierite zone. The exact location of this reaction can only be bracketed between the garnet + cordierite and the cummingtonite + cordierite isograds.

Reaction(4) represents the cummingtonite + cordierite isograd delineated on Figure 2.

The hypersthene isograd (Fig. 2), located near the Stillwater Complex, is based on reaction (5). This reaction involves the simple dehydration of cummingtonite to form hypersthene.

Throughout the garnet + cordierite zone four-phase assemblages are common. The univariant assemblages generally contain garnet + anthophyllite + cordierite + staurolite. This assemblage represents the reactants and products of a univariant reaction, reaction (3). In order for the these univariant assemblages to be stable in P-T space, they must lie on a univariant reaction curve as represented by reaction (3). The five-phase assemblage represented on Figure 3B contains gedrite + cordierite + chlorite + garnet + staurolite.

Since gedrite is present, the assemblage becomes univariant by the addition of a fourth component, Na2O. The presence of univariant assemblages in the garnet + cordierite zone indicates that the chemical potential of H2O has been buffered by the rock.

Gedrite-bearing assemblages are somewhat problematic. These assemblages are generally of low-variance and must be represented graphically by the addition of an extra component. The high Na2O component of the gedrites from the Boulder River Complex precludes a graphical representation on the AFM plane. In all assemblages which contain gedrite, a graphical representation on the AFM plane creates crossing tie lines. When Na2O is added to the system, the tie lines no longer cross; therefore, sodium-rich gedrites should not be plotted on the AFM plane. Furthermore, the phase relationships of gedrite are not well understood and further work on this subject is necessary.

The development of the petrogenetic grid based on naturally occurring assemblages is a major goal in metamorphic petrology. Spear (1977) and Robinson and Jaffe (1969) developed petrogenetic grids for assemblages similar to those seen in the Boulder River complex. The petrogenetic grid constructed by Robinson and Jaffe (1969) uses mineral compositions that are similar to those measured in the Boulder River complex.

Since the slopes of univariant lines in P-T space are composition dependent, the petrogenetic grid constructed by Robinson and Jaffe better describes the reaction relationships seen in the pelitic rocks of the Boulder River complex.

Reactions inferred from the AFM diagram (Fig. 3) are not significantly different from those described by Robinson and Jaffe (1969, 1969b). Figure 3B and 3C indicate that staurolite + gedrite + cordierite + garnet are stable in a portion of the Boulder River complex. The divariant field I in Figure 9 has the facies type illustrated in Figure 8C and is bound by the univariant reactions presented by Robinson and Jaffe (1969):

$$cm + st = anth + ga + qtz + H2O$$

$$anth + ky + H2O = cd + st + H2O$$

$$anth + st + qtz = cd + ga + H2O$$

The later reaction is observed to have occurred throughout the garnet + cordierite zone, and divariant field II in Figure 9 is represented by the same facies type as field I except the garnet + cordierite tie line is stable instead of the staurolite + anthophyllite tie line.

The next observed reaction, reaction (5), relates divariant field II to divariant field III (Fig. 9), which is represented by the facies type illustrated in Figure 8D and is bound by the univariant reactions:

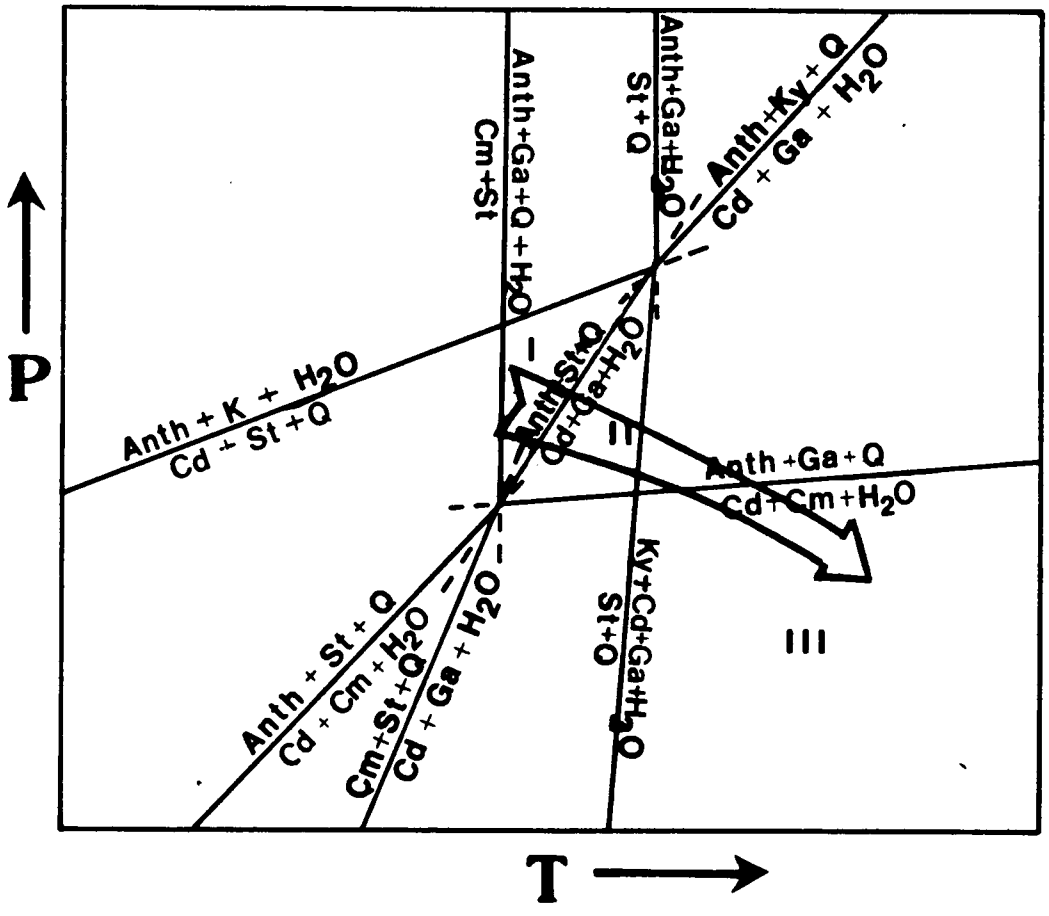

Figure 9. Petrogenetic grid taken from Robinson and Jaffe (1969) showing the reaction path of prograde metamorphism of the Boulder River Complex.

anth + ga + qtz = cm + H2O

st + qtz = ky + cd + ga + H2O

The reactions bracket a relatively narrow pressure range and a larger temperature range. Assuming that the Stillwater complex was emplaced as a horizontal sheet, the temperature increase toward the contact should occur with a nearly constant pressure. Based on this assumption, the proposed reaction path is indicated on Figure 9. The reaction path is generally isobaric as temperature increases. The highest grade divariant field contains ky + cd + ga and cd + cm. Due to the relatively low pressures and high temperatures, sillimanite is the stable aluminosilicate polymorph rather than kyanite.

The metamorphic history of the metamorphosed rocks beneath the Stillwater Complex has been debated among many authors. Evidence for both a polymetamorphic and single metamorphic event are seen throughout the Boulder River complex. The timing of fault movement(s) on the Mill Creek-Stillwater fault zone is relatively well constrained since the Stillwater Complex is displaced on its southeastern margin by the Mill Creek-Stillwater fault zone. Previous authors (Page, 1977; Hess, 1960; and many others) working in the Stillwater Complex have not seen any evidence of metamorphic foliations preserved in the Stillwater intrusion.

These constraints indicate the Stillwater Complex was emplaced possibly during the late stages of metamorphism and prior to fault movement(s) along the Mill Creek-Stillwater fault zone.

The strongly foliated rocks throughout the Boulder River valley appear as regionally metamorphosed graywackes and argillites. The foliation in the vicinity of the major fault zones can be attributed to tectonic movement. This mechanism can be called upon to describe the foliations near fault zones; however, a pervasive foliation is observed far from the major fault zones in the Boulder River valley.

Temperatures indicated from geothermometers increase as the Stillwater Complex is approached. Garnet/biotite and garnet/cordierite geothermometry yield temperatures from ~430 to ~750°C in the contact aureole. Inverted pigeonite in the Stillwater iron-formation indicates a minimum temperature of ~825°C near the Stillwater contact. The temperatures from garnet/biotite and garnet/cordierite are ~100°C lower than temperatures indicated by pigeonite in the iron-formation. Labotka (1985) proposed that the temperatures recorded by the garnet-bearing assemblages may be the result of reequilibration at lower than peak metamorphism.

The high temperatures at the contact and unusually high temperatures from greater than 7 km from the contact suggest an ambient temperature at the time of emplacement of the Stillwater Complex was in the vicinity of 400 ^{o}C (Labotka, 1985). This figure was determined by assuming conductive cooling of a magma emplaced at 1200 ^{o}C. The temperature at the contact is approximately the mean of the magma temperature and the country rock ambient temperature (Labotka, 1985).

The lack of any metamorphic foliations in the Stillwater Complex indicates the Stillwater intrusion was not metamorphosed. The increasing thermal gradient toward the Stillwater Complex indicates that the source of heat during metamorphism was from the Stillwater intrusion. The age of the Stillwater Complex is 2700 my as determined by Depalo and Wasserburg (1979), and the age of the metamorphic rocks in the Boulder River valley is 2730 +/- 30 my as determined by Powell et al. (1969). The strong correlation indicates that the Stillwater Complex either reset the Rb-Sr clock in the pelitic rocks of the Boulder River valley or that the Stillwater Complex intruded during a regional metamorphic event.

Weeks (1980) and Mogk (1985, personal communication) have suggested that the contact between the hornfelses and the schists is a fault contact.

Petrographic and field evidence observed by this author indicate that no fault is present, and the contact is totally gradational. Samples from the northeast side of this presumed fault, in the cummingtonite + cordierite zone of the Stillwater hornfels, contain relict foliations. If the contact metamorphism is truly superimposed on a schistose terrain, the relict foliations in the cummingtonite + cordierite zone indicate a fault could not exist between the hornfelses and the schists. The "transitional" zone between the hornfelses and the schists was crossed many times during sample collection and no evidence of shearing or faulting was seen.

The gradational transition from the Stillwater hornfels to the Boulder River schist, combined with temperature and pressure estimates, indicates that the Stillwater intrusion was emplaced at 7 to 12 km into a regionally metamorphosed terrain during late stages of metamorphism. The contact metamorphic effects appear to have been superimposed on a nearly contemporaneous regionally metamorphosed terrain.

REFERENCES

REFERENCES CITED

Albee, A.L., and Ray, L., 1970, Correction factors for electron probe microanalysis of silicates, oxides, carbonates, phosphates, and sulfates: Analytical Chemistry, v. 42, p. 1408-1414.

Bence, A.E., and Albee, A.L., 1968, Emperical correction factors for the electron microanalysis of silicates and oxides: Journal of Geology, v. 76, p. 382-403.

Butler, J.R., 1965, Contact metamorphism along the base of the Stillwater Complex, Montana: Geol. Soc. America Spec. Paper 82, p. 24.

Butler, J.R., 1966, Geologic evolution of the Beartooth Mountains, Montana and Wyomong: Pt. 6, Cathedral Peak area Montana: Geological Society of America Bulletin, v. 77, p. 45-64.

Cassella, C.J., 1964, Geologic evolution of the Beartooth Mountains, Montana and Wyoming. Part 4. Relationship between Precambrian and Laramide structures in the Line Creek area:Geol. Soc. America Bull., v. 75, p. 969-986

DePalo, D.J., and Wasserburg, G.J., 1979, Sm-Nd age of the Stillwater Complex and the mantle evolution curve for neodymium: Geochim. Cosmochim. Acta v. 43, no. 7, p. 999-1008.

Eckelmann, F.D., and Poldervaart, Arie, 1957, Geologic evolution of the Beartooth Mountains, Montana and Wyoming. Partl. Archaean history of the Quad Creek area: Geol. Soc. America Bull., v. 68, p. 1225-1262.

Ferry, J.M., and Spear, F.S., 1978, Experimental calibration of the partitioning of Fe and Mg between biotite and garnet: Contrib. Mineral Petrol., v. 66,p.113-117

Fonarev, V.I., and Korolkov, 1980, The assemblage orthopyroxene + cummingtonite + quartz. The low-temperature stability limit:Contrib. Mineral. Petrol., v. 73, p. 413-420.

Foose, R. M., Wise, D.V., and Gabbarina, G.S., 1961, Structural geology of the Beartooth Mountains, Montana and Wyoming: Geological Society of America Bulletin, v. 72, p. 1143-1172.

Goldman, D.S., and Albee, A.L., 1977, Correction of Fe/Mg partitioning between garnet and biotite with 180/160 partitioning between quartz and magnetite: American Journal of Science, v. 277, p. 750-767.

Harris, R.L., 1959, Geologic evolution of the Beartooth mountains, Montana and Wyoming. Part 3. Gardner Lake area, Wyoming: Geol. Soc. America Bull., v. 70, p. 1185-1216.

Hemely, J.J., Montaya, J.W., Shaw, D.R., and Luce, R.W., Mineral equilibria in the MgO-SiO2-H2O system: II. talc antigorite- forsterite - anthophyllite - enstatite stability relations and some geological implications in the system: Am. Journal Science, v. 277, p. 253-383.

Henson, B.J., and Green, D,H., 1971, Experimental study of the stability of cordierite and garnet in pelitic compositions at high pressures and temperatures, II. Compositions without excess alumino silicate:Contrib. Mineral. Petrol., v. 35, p. 331-354.

Hess, G.B., 1960, Stillwater igneous complex, Montana--a qunatitative mineralogical study: Geological Society of America, Memoir 132, p. 503-520.

Holdaway, M.J., 1971, Stability of andalusite and the aluminum silicate diagram:American Journal of Science, v. 271, p. 97-131.

Holdaway, M.J., and Lee, S.M., 1977, Fe-Mg cordierite stability in high-grade pelitic rocks based on experimental, theoretical, and natural abservations: Contrib. Mineral. Petrol., v. 63, p. 175-198.

Jackson, E.D., 1961, Primary textures and mineral associations in the ultramafic zone of the Stillwater Complex, Montana: U.S. Geological Survey Prof. Paper 358.

Jackson, E.D, Howland, A.L., Peoples, J.W., and Jones, W.R., 1954, Geologic maps and sections of the eastern part of the Stillwater Complex in Stillwater County Montana: U.S. Geological Survey Open-file Report.

Jones, W.R., Peoples, J.W., and Howland, A.L., 1960, Igneous and tectonic structures of the Stillwater Complex, Montana: U.S. Geological Survey Bulletin 1071-H, p. 281-340.

Labotka, T.C., 1985, Petrogenesis of the metamorphic rocks beneath the Stillwater Complex: Assenblages and conditions of metamorphism: in press.

Labotka, T.C., Vaniman, D.T., and Papike, J.J., 1982, Contact metamorphic effects of the Stillwater Complex, Montana: the concordant iron formation. A reply to the role of buffering in the metamorphism of the iron formation: American Mineralogist v. 67, p. 149-152.

Lammars, E.C., 1939, Precambrian control of Laramide structures in the Beartooth Range, Montana and Wyoming (abs): Geol. Soc. America Bull., v. 50, p. 1918.

Lindsley, D.H., 1983, Pyroxene thermometry: American Mineralogist, v. 68, p. 477-493.

Martignole, J. and Sisi, J.C., 1981, Cordierite-garnet-H2O equilibrium: a geological thermometer, barometer, and water fugasity indicator: Contrib. Mineral. Petrol.,v. 77,p. 38-46.

Newton, R.C., 1972, An experimental determination of the high pressure stability limits of magnesian cordierite under wet and dry conditions: J. Geology, v. 80, p. 398-420.

Newton, R.C., 1983, Geobarometry of high-grade metamorphic rocks: American Journal of Science, v. 283-A, p. 1-28.

Newton, R.C., and Perkins, III, D., 1982, Thermodynamic calibration of geobarometers based on the assemblages garnet-plagioclase-orthopyroxene-(clinopyroxene)-quartz: American Mineralogist, v. 67, p. 203-222.

Newton , R.C., and Wood, B.J., 1979, Thermodynamics of water in cordierite and some pertologic conquences of cordierite as a hydrous phase:Contirb.Mineral.Petrol., v. 68, 391-405.

Page, N.J., 1977, Stillwater Complex, Montana, rock secession, metamorphism and structure of the complex and adjacent rocks: U.S. Geological Survey Prof.Paper 999, p. 79.

Page, N.J., and Nokleberg, W.J., 1972, Genesis of mesozonal granitic rocks below the base of the Stillwater Complex in the Beartooth Mountains,Montana: U.S. Geological Survey Prof. Paper 800-D, p.D127-D141.

Page, N.J., Simons, F.S., and Dohrenwend, J.C., 1973a, Reconnaissance geologic map of the Mt. Douglas quadrangle, Montana: U.S. Geological Survey Miscellaneous Field Investigations Map MF 491.

Podpora, C., and Lindsley, D.H., 1979, Fe-rich pigeonites: minimum temperature of stability in the Ca-Mg-Fe quadrilateral (abs) :EOS, v. 60, p. 420-421.

Powell, J.L., Skinner, W.R., and Walker, D., 1969, Whole-rock Rb-Sr age of the metasedimentary rocks below the Stillwater Complex, Montana: Geological Society of America Bulletin, v. 80, no. 8, p. 1605-1612.

Richardson, S.W., 1968, Staurolite stability in a part of the system Fe - Al - Si - O - H: J. Petrol., v. 9, p. 467- 488

Robinson, P., and Jaffe, H.W., 1969b, Aluminous enclaves in gedrite-cordierite gneiss from southwestern New Hampshire: American Journal of Science, v.267,p.389-421.

Robinson, P. and Jaffe, H.W., 1971, Composition of the anthophyllite-gedrite series, comparison of gedrite and hornblende, and the anthophyllite-gedrite solvus: Am. Mineralogist, v. 56, p. 1005-1039.

Robinson, P. and Jaffe, H.W., 1969, Chemographic exploration of amphibole assemblages from central Massachusetts and southwestern New Hampshire: Mineral Society of America Special Paper 2, p.251-274.

Spear, F.S., 1978, Petrogenetic grid for amphibolites from the Post Pond Volcanics: Carnegie Institute of Washington Year Book 67, p. 805-808.

Spear, F.S., 1980, The gedrite-anthophyllite solvus and the composition limits of orthoamphibole from the Post Pond Volcanics, Vermont: American Mineralogist, v. 65, p. 1103-1118.

Spear, F.S., 1982, Phase equlibria of Amphibolites from the Post Pond Volcanics, Mt. Cube Quadrangle, Vermont: Journal of Petrology, v.23, p. 383-426

Spencer, E.W., 1959, Geologic evolution of the Beartooth Mountains, Montana and Wyoming. Part 2. Fracture patterns: Geological Society of America Bulletin, v. 70, p. 467-508.

Stout, J.H,, 1972, Phase petrology and mineral chemistry of coexisting amphiboles from Telmark, Norway: Journal of Petrology, v. 13, p. 99-145.

Thompson, A.B., 1976, Mineral reactions in pelitic rocks: I. Prediction of P-T-X(Fe-Mg) phase relations: American Journal of Science, v. 276, p. 401-424.

Thompson, A.B., 1976, Mineral reactions in pelitic rocks: II. Calculations of some P-T-X(Fe-Mg) phase relations: American Journal of Science, v. 276, p. 425-454.

Thompson, J. B., 1957, The graphical analysis of mineral assembalges in pelitic schists: American Mineralogist, v. 42, p. 842-858.

Vaniman, D.T., Papike, J.J., and Labotka, T.C., 1980, Contact-metamorphic effects of the Stillwater Complex, Montana, the concordant iron formation: American Mineralogist, v. 65, no. 11-12, p. 1087-1102.

Vaniman, D.T., Labotka, T.C., and Papike, J.J., 1979, Pyroxene constraints on the thermal history of the Stillwater iron-formation, Montana: Eos (American Geophys. Union, Trans.), v. 60, p. 422.

Vocke, C.M., 1982, T-fO2 conditions of the metamorphism of the Stillwater iron-formation, Montana: State University of New York M.S. Thesis.

Weeks, G., 1980, Precambrian geology of the Boulder river area, Beartooth Mountains, Montana: Missoula, MT, University of Montana, Master's Thesis, p. 58.

Wise, D.U., 1958, The relationship of Precambrian and Laramide structures in the southern Beartooth Mountains, Wyoming: Billings Geol. Soc. Guidbook 9th Ann. Field Conf., p. 24-30.

Zen, E-an, 1961, Components, phases, and criteria of chemical equilibrium in rocks: American Journal of Science, v. 261, p. 929-942.

Zientek, M.L., (in press)

APPENDIX

Bulk Rock Analyses of Selected Samples from the Boulder River Complex

Analytical Technique

Whole rock chemistry was determined on selected samples using an ORTEC EG&G tube excited x-ray fluoerescence. Copper and Indium filters were used for approprate elements. Samples used for the analyses were taken from thin section chips of the microprobe samples and were pulverized to a fine powder in a tungsten carbide shatter box. Pellets were backed with boric acid and pressed at 30,000 psi. Precision was monitored by analyzing U. S. Geological Survey whole rock standards of known composition. Measured precision is $< 3\%$ for major elements, except Mg and Na, and $< 10\%$ for minor elements.

Table A-IX

X-Ray Fluorescence Whole Rock Analyses of selected samples

Sample #	44	91	109	129	146	169	174
SiO2	58.210	54.430	61.020	51.120	54.700	54.540	53.640
TiO2	0.580	0.807	0.641	0.760	0.712	0.734	0.700
Cr	0.045	0.079	0.069	0.079	0.074	0.053	0.078
Al203	16.600	20.290	15.820	20.380	18.730	18.950	18.260
Fe203	9.200	12.270	10.830	11.930	11.650	10.950	13.970
MnO	0.118	0.108	0.107	0.118	0.129	0.163	0.134
MgO	5.767	7.120	5.971	8.136	7.277	7.179	6.929
CaO	2.366	0.412	0.666	0.211	0.497	1.039	0.471
Na20	2.247	0.808	1.033	1.309	1.036	1.481	1.344
K20	2.069	2.234	1.749	2.802	2.683	3.378	2.135
V	0.008	0.011	0.009	0.014	0.011	0.011	0.012
Ni	0.016	0.030	0.026	0.034	0.031	0.019	0.028
Rb	0.011	0.008	0.007	0.011	0.010	0.011	0.008
Sr	0.015	0.004	0.007	0.003	0.004	0.009	0.005
Y	0.002	0.004	0.001	0.002	0.002	0.002	0.002
Zr	0.012	0.009	0.007	0.008	0.009	0.009	0.008
Nb	0.001	0.001	0.007	0.001	0.001	0.001	0.001
Total	97.260	98.620	97.960	96.920	97.560	98.530	97.700

VITA

Randal Lee Kath was born in Minneapolis, Minnesota on August 10, 1961. He attended elementary school in Georgia and Florida and was graduated from Riverwood High School, Atlanta, Georgia, in March 1979. The following September he entered Southern Technical Institute. The following September he entered West Georgia College in Carrollton, Georgia, and in June 1984 he received a Bachelor of Science degree in Geology. In the fall of 1984 he accepted a teaching assistantship at The University of Tennessee, Knoxville and began to study toward a Master's degree. This degree was awarded in August 1986.

The author is entering the Graduate School of The South Dakota School of Mines and Technology, Rapid City South Dakota, in January of 1987.